Geoderma 443 (2024) 116818

Contents lists available at ScienceDirect

Geoderma

journal homepage: www.elsevier.com/locate/geoderma

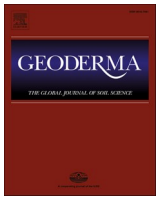

Quantification of soil organic carbon in particle size fractions using a near-infrared spectral library in West Africa

Aurélie Cambou [a,*], Issiakou A. Houssoukpèvi [a,b], Tiphaine Chevallier [a], Patricia Moulin [c], Nancy M. Rakotondrazafy [a], Eltson E. Fonkeng [d,e], Jean-Michel Harmand [a,d,f,g], Hervé N.S. Aholoukpè [b,h], Guillaume L. Amadji [b], Fritz O. Tabi [e], Lydie Chapuis-Lardy [a], Bernard G. Barthès [a]

[a] *Eco&Sols, Université de Montpellier, CIRAD, INRAE, IRD, Institut Agro Montpellier, France*
[b] *Université d'Abomey-Calavi, Cotonou, Benin*
[c] *Imago, IRD, Dakar, Senegal*
[d] *CIRAD, UMR Eco&Sols, Montpellier F-34398, France*
[e] *University of Dschang, Dschang, Cameroon*
[f] *CIRAD, UMR Eco&Sols, Yaoundé, Cameroon*
[g] *World Agroforestry, Yaoundé, Cameroon*
[h] *Centre de Recherches Agricoles Plantes Pérennes (CRA-PP), Institut National des Recherches Agricoles du Bénin, Pobè, Benin*

ARTICLE INFO

Handling Editor: B. Minasny.

Keywords:
Standard error of laboratory
Soil organic matter pools
Locally weighted partial least squares regression
Diffuse reflectance spectroscopy
Spiking

ABSTRACT

Particle size fractionation enables a better understanding of soil organic carbon (C) dynamics since it separates fractions that differ in composition, residence time and function. However, this method is time-consuming and tedious; thus, its use has been greatly limited. Our objective was to evaluate the ability of an existing soil spectral library (SSL) from different regions of West Africa to predict the C amount in the fractions (gC kg^{-1} soil) of the samples in a new target set from Benin.

The SSL included 181 samples from five countries, and the target set included 94 samples (depth $\leq$ 40 cm), most of which were coarse-textured; near-infrared reflectance (NIR) spectra were collected for 2 mm sieved samples (non-fractionated samples). The predicted variables were the C amounts in the non-fractionated soil and in the $<$ 20, 20–50, and $>$ 50 μm fractions (F$<$20, F20–50, and F$>$50, respectively). Different methods were tested to optimize the predictions: (i) SSL enrichment with 10 or 15 samples selected from the target set (spiking) and replicated six times (i.e. extra-weighted); (ii) locally weighted (local) partial least squares regression (PLSR), which is calibration by the spectral neighbours with the highest weights attributed to closest neighbours, and was compared to "global" (i.e., common) PLSR, where all calibration samples equally contribute; and (iii) spectrum pretreatments (e.g., smoothing, centring, derivatization). In addition, the intermediate precision of the conventional data (standard error of laboratory; SEL_{int}) was estimated through triplicate fractionation of three samples carried out by three operators (one per replicate).

When the SSL alone was used for calibration, the predictions were inaccurate for the C amounts in the non-fractionated soil and in F$<$20; however, the predictions were accurate for the C amounts in F20-50 and F$>$50, with minimal benefit from the local PLSR over the global PLSR in general. For the non-fractionated soil, F$<$20, F20–50 and F$>$50, the ratios of performance to the interquartile range in the validation set, $RPIQ_{VAL}$, were 1.6–1.8, 1.6–1.7, 1.9 and 1.9–2.1, respectively. Calibration with SSL spiked (i.e., completed with spiking samples) yielded an increase in $RPIQ_{VAL}$ from 33 to 56% for the C amount in the non-fractionated soil and F$<$20 and from 0 to 20 % for F20-50 and F$>$50 ($RPIQ_{VAL}$ reached 2.4–2.5, 2.2–2.3, 1.9–2.0 and 2.1–2.3, respectively), and the benefit of local PLSR was still limited. The SEL_{int} was based on a few samples and thus only provided a rough estimation; this estimate represented at least 65% of the prediction error for the C amounts in the fractions. Therefore, the SEL_{int} needs to be determined more extensively to both improve the model accuracy and refine the interpretation of the predictions based on NIR spectra. This library should be enriched with samples from other sites to represent other soil types.

* Corresponding author at: UMR Eco&Sols, Institut Agro, 2 Place Viala, bât. 12, Cedex 2, Montpellier 34060, France.
E-mail address: aurelie.cambou@ird.fr (A. Cambou).

https://doi.org/10.1016/j.geoderma.2024.116818
Received 21 August 2023; Received in revised form 12 February 2024; Accepted 13 February 2024
Available online 22 February 2024

1. Introduction

Soil organic matter (SOM) contributes to the maintenance of soil physical (e.g., soil aeration and aggregation), chemical (e.g., pH regulation and nutrient reserve), and biological functions (e.g., through soil organism activities; Lal, 2014). Moreover, soil organic carbon (SOC) sequestration appears to be a solution for limiting the ongoing increase in the atmospheric carbon dioxide (CO_2) concentration (e.g., Dignac et al., 2017; "4 per 1000" Initiative, 2018). Thus, enhancing or at least maintaining the SOM stock, which is made up of at least 50% of SOC, is crucial considering its essential role in the ability of soils to provide ecosystem services (e.g., biomass supply and climate change mitigation).

However, SOM is very complex and includes multiple compounds with contrasting C inputs, dynamics and responses to disturbances. Many methods of SOM fractionation have been developed to separate SOM pools that are as homogeneous and distinct as possible in terms of their dynamics and resilience in soils (von Lützow et al., 2007; Moni et al., 2012; Poeplau et al., 2018). Among these methods, the physical fractionation of particles according to their size and/or density reveals the importance of interactions between organic and inorganic soil components in SOM turnover and has been considered a particularly relevant fractionation approach (Balesdent, 1996; Christensen, 2001; Lavallee et al., 2020). This physical approach enables the differentiation of two radically different pools in terms of composition, residence time and functioning: (i) light and coarse particulate SOM (POM; one or two fractions >50 μm according to the fractionation protocol), which has predominantly a vegetal signature, is assumed to have high turnover rate and is relatively undecomposed and vulnerable to land use change; and (ii) finer mineral-associated SOM (MAOM; from one to four fractions < 50 μm according to the protocol), generally with slow turnover due to chemical bonding to minerals and physical protection in fine aggregates (Lehmann and Kleber, 2015; Cotrufo et al., 2019; Lavallee et al., 2020).

However, conventional methods for physical SOM separation are time-consuming and tedious, which limits the monitoring of SOC dynamics in space and time at the regional or territorial scale. Infrared spectroscopy, coupled with chemometrics, represents an alternative to conventional analytical methods for assessing soil properties; its cost- and time-effectiveness has been demonstrated for quantifying SOC and nitrogen contents (Stenberg et al., 2010; O'Rourke and Holden, 2011). Several studies have also shown the ability of near-infrared diffuse reflectance spectroscopy (NIRS), visible and NIRS (VNIRS) or mid-infrared reflectance spectroscopy (MIRS) applied to bulk soil (non-fractionated soil; < 2 mm) to predict the size of the SOC pools obtained with different fractionation methods (Zimmermann et al., 2007; Barthès et al., 2008; Yang et al., 2012; Baldock et al., 2013; Jaconi et al., 2019; Greenberg et al., 2022; Ramifehiarivo et al., 2023). Barthès et al. (2008) particularly studied the ability of NIRS to predict the SOC distribution in particle size fractions. Their work showed encouraging prediction results for the finest MAOM studied (0–20 μm fraction; F<20). This SOC fraction is particularly interesting to predict because, on the one hand, it is one of the most difficult fractions to separate (obtained at the last stages of the fractionation process), and on the other hand, it is the predominant SOC fraction in most soils (Feller and Beare, 1997; Pansu and Gautheyrou, 2006a; Barthès et al., 2008). However, in previous studies, the calibration set, which is used to build the prediction model, and the validation set, which is used to test the model, were not specifically selected to be location-independent; therefore, the prediction results could be overly optimistic (Brown et al., 2005). Since the first use of infrared spectroscopy to characterize soil properties, many soil spectral libraries (SSLs) have been built as parts of different projects within research laboratories. In particular, several wide-scale SSLs have been built and used to predict the SOC content or other soil properties on local or geographically independent target sample sets (Guerrero et al., 2010; Gogé et al., 2014; Barthès et al., 2020; Gomez et al., 2020; Li et al., 2020). Due to the tediousness and cost of SOC physical fractionation (labour time, analysis price of each SOC fraction), all the existing databases that include data on SOC fractions and bulk soil spectra should be pooled together. Then, this pooled SSL could be used to make predictions on new target sample sets, thus, avoiding the additional time-consuming work involved in fractionation. Moreover, this approach would add value to the existing SOC fractionations, as these would help predict SOC fractions in new samples. However, to date, no study has tested the ability of models calibrated on existing SSLs to accurately predict SOC pools on new, geographically independent sample sets. To fit infrared spectra to soil properties, different multivariate regression procedures can be used, such as partial least squares regression (PLSR); PLSR is commonly used due to its efficiency, interpretability and low computation time (Angelopoulou et al., 2020; Barthès and Chotte, 2020). PLSR has most often been used in "global" calibration, where all calibration samples contribute equally to model development. However, several studies have demonstrated the benefits of calibration by spectral neighbours, often called "local" calibration, especially when using wide-scale calibration SSL for predictions on independent target sets (Barthès et al., 2020; Cambou et al., 2021; Mallet et al., 2022). Guerrero et al. (2014) showed that spiking and extra-weighting could improve model accuracy when validation was performed on an independent target sample set: spiking consists of enriching the calibration database with few samples from the target set, and extra-weighting consists of artificially replicating these spiking samples to increase their influence on the calibration. Barthès et al. (2020) compared the performances of global and local calibrations and studied the benefits of spiking and extra-weighting for predicting soil inorganic carbon (SIC) content via MIRS. They showed that spiking with extra-weighting was more useful for global than for local calibration and that the best predictions were obtained with local calibrations. The performance of global vs. local calibration, with or without spiking and extra-weighting, still needs to be studied for other variables and other spectral ranges.

In the present study, databases from previous studies (1998–2019) were used; these included the following: (i) SOC physical fractionation results obtained with the same methodology and (ii) NIR spectra acquired on non-fractionated soil using the same spectrometer (Foss NIRSystems 5000, Laurel, MD, USA). However, these procedures were carried out by different operators at different times. The objectives of the present study were as follows:

- to optimize the predictions of SOC in the particle size fractions of a regional target sample set in Benin (94 samples studied in 2019, collected at 0–10 cm and 10–30 cm depths) using a NIR SSL from West Africa (184 samples studied between 1998 and 2017 and collected from different depth layers in the top 40 cm);
- to compare the performance of global vs. local calibrations, with or without spiking and extra-weighting to predict the SOC fractions.

2. Materials and methods

2.1. Sample subsets included in the soil spectral library

The SSL included seven sample subsets originating from previous studies carried out from 1998 to 2017 in Burkina Faso, Republic of Congo (Congo-Brazzaville), Togo, Cameroon and Benin (Table 1, Fig. 1).

Two soil sample subsets were collected in Burkina Faso in 2008, and both were described by Barthès et al. (2008). Briefly, one set originated from Banh in northern Burkina Faso. The area was occupied by millet crops (with or without manure addition), and the soil type is mainly an Arenosol (IUSS Working Group WRB, 2015). This sample subset included 28 samples with depths ranging from 0–10 cm to 30–40 cm. The other sample subset originated from Torokoro in southern Burkina Faso. The soil type is a Lixisol (IUSS Working Group WRB, 2015). The studied land uses were crops (cotton, yam, sorghum), fallows, orchards and forests. This subset included 52 samples collected at a depth of 0–10

cm.

In 2008, another sample subset was collected at several sites near Pointe-Noire, in Congo-Brazzaville, where the soil type is an Arenosol. The studied land uses were eucalyptus plantations and savanna. This subset included 34 samples from a depth of 0–10 cm and was also described by Barthès et al. (2008).

One sample subset was collected in 2015–2016 in northern Togo, where the main soil type is Plinthosol (IUSS Working Group WRB, 2015). This subset included six soil samples collected at 0–5 and 20–30 cm depths under cereal crops or savanna.

One sample subset was collected in 2017 in the Bokito district located in central Cameroon, where the main soil type is Ferralsol (IUSS Working Group WRB, 2015). The studied land uses were savanna and different types of cocoa plantations, cultivated in monoculture or associated with shade trees. This subset included 38 composite soil samples collected at a depth of 0–10 cm. In shaded plantations, the sampling was carried out separately between the cocoa tree stems in the shade and between the unshaded cocoa tree stems. The detailed sampling design for this study was described by Sauvadet et al. (2020).

Two sample subsets were collected in southern Benin. The first study was carried out in 1998 at an experimental station near the village of Agonkanmey in the Atlantique administrative department (southern Benin). The main soil type is Nitisol (IUSS Working Group WRB, 2015). The following four experimental plots were studied: (i) yearly maize-mucuna association; (ii) maize-mucuna association with maize every year and mucuna every two years; (iii) continuous maize with mineral fertilization; and (iv) continuous maize with burning and no input (traditional system; Azontonde, 2000). In each plot, one composite sample was prepared from three elementary samples collected at a depth of 0–10 cm; thus, the subset included four 0–10 cm composite samples. The second sample subset was obtained from 2010 to 2013 from two mature oil palm tree plantations in the Plateau department (southeastern Benin). The main soil type is Nitisol. In these plantations, the pruned leaves were returned to the tree rows as windrows for approximately 10 years. The samples were collected at depths of 0–5 cm and 20–30 cm (i) under windrows in tree rows and (ii) in the inter-rows, in three 1-m deep pits in each case. This subset should have included 24 samples but fractionation results were not available for one 0–5 cm sample under a windrow, resulting in a total of 23 samples. This sample subset was precisely described by Aholoukpè (2013) and Aholoukpè et al. (2016).

The soil textures were mostly sandy, with some differences between the subsets; the textures were as follows: sandy for Cameroon, Togo, the Congo and both subsets from Burkina Faso; sandy loam or sandy clay loam for the subset from southern Benin; loamy sand for the topsoil (0–5 cm) samples from southeastern Benin; and sandy loam for the subsoil (20–30 cm) samples from the same subset.

2.2. Target set

The target set included soil samples from southwestern Benin in the Atlantic department (Houssoukpèvi et al., 2022; Table 1 and Fig. 1). The sampling was carried out in 2019 in three villages on the Allada plateau (Allada, Toffo and Zè); they cover 1500 km^2. The main soil type is Nitisol. The set included samples from two forest sites, two tree plantations (teak plantations of 5 and 21 yrs old), two adult oil palm groves

Table 1
Description of the soil sample sets used as spectral library and target set.

Location and year of conventional analysis	Mean annual rainfall and temperature	Climate classification[a]	Soil type[b]	Mean sand content (%)	Land use	Number of samples	Sample depth (cm)
Soil spectral library							
Banh, northern Burkina Faso 14°04′N, 02°26′W 2008	600 mm 29 °C	BSh	Ferralic Arenosols	73	Millet with or without manure addition (corralling)	28	0–10 to 30–40
Torokoro, southern Burkina Faso 10°03′N, 04°25′W 2008	1100 mm 27 °C	Aw	Haplic Lixisols	80	Cotton, sorghum, yam, fallow, orchard, forest	52	0–10
Pointe-Noire, Congo-Brazzaville 04°S, 12°E 2008	1200 mm 25 °C	Aw	Ferralic Arenosols	93	Eucalyptus plantations, savanna	34	0–10
Savanna Region, northern Togo 11°01′-02′N, 00°08′-14′E 2015–2016	1050 mm 29 °C	Aw	Pisoplinthic Plinthosols	75	Cereals, savanna, forest	5[c]	0–5 and 20–30
Bokito district, Cameroon 04°30′N, 11°10′E 2017	1400 mm 25 °C	Aw	Orthic Ferrasols	81	Cocoa in monoculture or in agroforestry, savanna	38	0–10
Agonkanmey, southern Benin 06°24′N, 02°20′E 1998	1100 mm 27 °C	Aw	Dystric Nitisol	77	Maize with possible legume cover crop (mucuna)	4	0–10
Plateau district, southeastern Benin 06°45′-49′N, 02°37′-38′E 2010–2013	1300 mm 27 °C	Aw	Dystric Nitisols	80	Palm tree plantations	20[c]	0–5 and 20–30
Target set							
Allada plateau, southwestern Benin 06°20′-50′N, 02°00′E 2019–2020	1100 mm 27 °C	Aw	Dystric Nitisols	85	Palm tree plantations, maize, pineapple, forest	94	0–10 and 10–30

[a] Köppen-Geiger climate classification (Rubel and Kottek, 2010): Aw refers to tropical savanna climate and BSh to hot semi-arid climate.
[b] IUSS Working Group WRB (2015).
[c] after outlier removal.

(10–12 yrs old), two young oil palm groves (ca. 5 yrs old, both in temporary agroforestry, with maize and pineapple, respectively), and two croplands (maize and pineapple). Before cropping, the vegetation was often burnt, and the soil was subsequently hoed to a depth of 20 cm; moreover, mineral fertilizers were applied to the pineapple crop. In adult palm groves, pruned leaves were usually returned to the soil as windrows in the tree rows, and in this case, the soils under windrows and in the inter-rows were separately sampled. The soil samples were collected at 0–10 and 10–30 cm depths. In each studied plot and for each depth layer, one soil sample was collected in a hand-dug pit using a knife, and composite samples were also prepared from elementary samples collected all over the plot using a manual auger; this process led to a total of 96 fractionated samples. However, the fractionation results were not available for two samples, resulting in a total of 94 samples. All samples from this target set were sandy.

2.3. Determination of the C amount in the fractions and in the non-fractionated soil

All samples were initially air dried, gently crushed using a mortar and pestle, and subsequently sieved through a 2-mm mesh. For all sample sets, the fractionation methods used were adapted from Feller (1979), Balesdent et al. (1991) and Gavinelli et al. (1995); the fractionation was carried out by different operators at different times. Most of the studies performed particle size and density fractionation (the three sets from Benin and the sets from Cameroon and Togo). However, only particle size fractionation was performed for sample sets from Burkina Faso and the Congo.

For all sample sets, an aliquot (between 15 g for fine- or medium-textured soil samples and 40 g for sandy samples) of each 2-mm sieved, air-dried soil sample was immersed in a solution of deionized water and sodium hexametaphosphate (HMP; concentration of 1.7–2.5 g HMP L^{-1} water). After overnight soaking, the suspension was shaken with agate beads in a rotary shaker (40–50 rpm) for several hours, with the exception of the suspensions prepared with Benin southeastern samples; these were directly shaken without overnight soaking. For all sample sets, two wet sieving sequences were then carried out at 200 and 50 μm. After each wet sieving, the fraction retained on the sieve was collected, and for the particle size and density procedure only, the POM was separated from the heavier fraction by repeated floatation panning and sedimentation of mineral particles in water. The particle size and density procedure yielded four fractions > 50 μm: (i) the POM with a

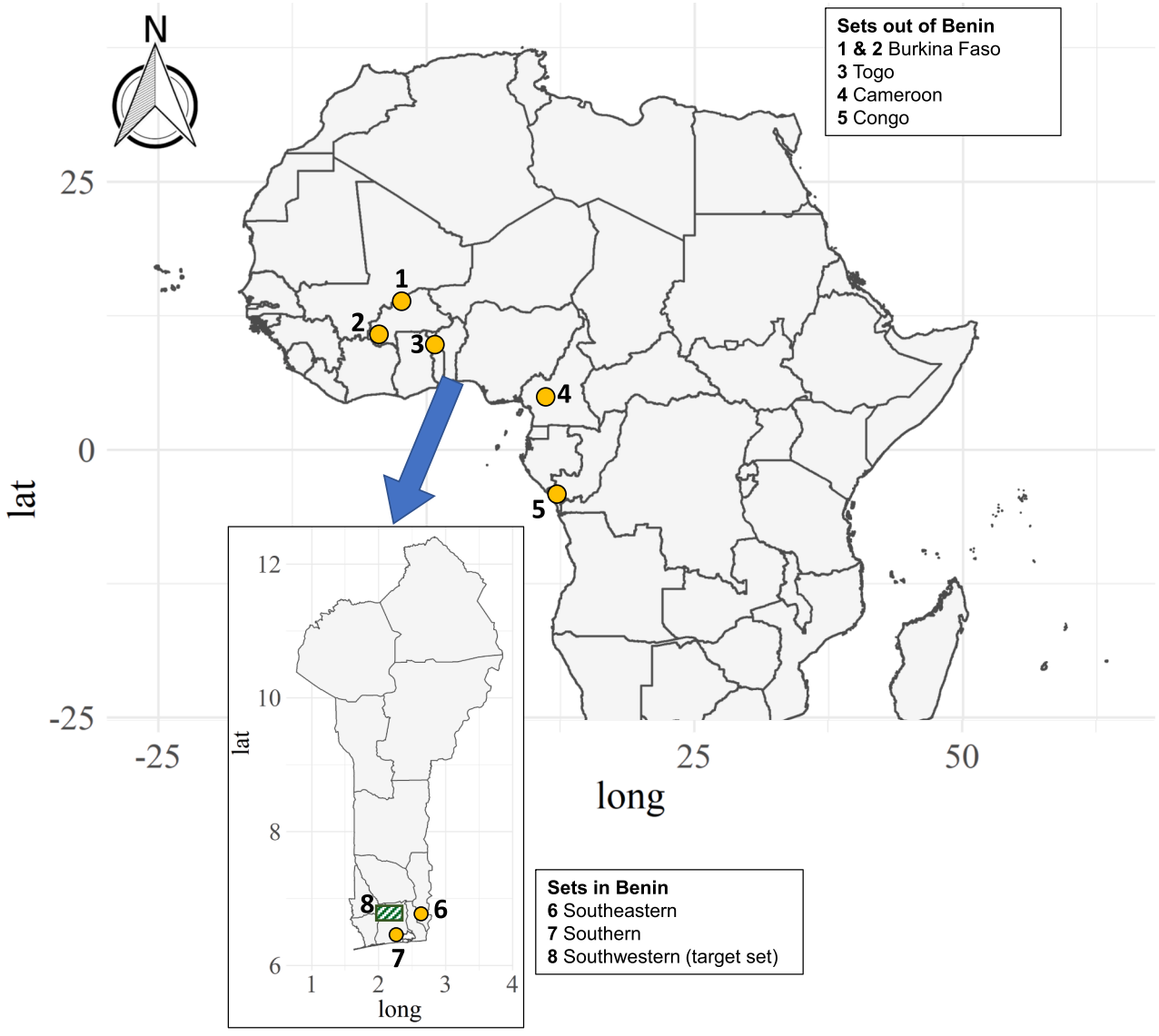

Fig. 1. Location of sampled sites in and out of Benin. The yellow circles represent the locations of the soil spectral library sites and the grid rectangle is the location of the target set. Spatial layers come from openAFRICA website (https://africaopendata.org/) and https://benin.gep.kartoza.com/.

size of 200–2000 μm, (ii) the 200–2000 μm heavy fraction, (iii) the 50–200 μm POM, and (iv) the 50–200 μm heavy fraction. In contrast, the particle size fractionation yielded only two fractions > 50 μm: the 200–2000 and 50–200 μm fractions (both including the heavy fraction and POM). Then, ultrasonication was applied to the suspension < 50 μm for 10 min using an ultrasonic processor working at operating/interruption intervals (Fisher Bioblock Scientific, Illkirch, France). Then, the 20–50 μm fraction (F20-50) and F<20 were separated by wet sieving at 20 μm, except for the samples from southeastern Benin; these were extracted by sedimentation in water. Depending on the period and on the soil, especially its texture, some parts of the fractionation procedure might have varied to some extent, but the objective was always to achieve maximal dispersion of elementary particles with minimal alteration of SOM and especially POM. Thus, it was assumed that the slight differences in procedure did not noticeably affect the results. Fractionation was also carried out after SOM destruction using hydrogen peroxide (H_2O_2; i.e., usual particle size analysis, which is actually a size analysis of mineral particles; Pansu and Gautheyrou, 2006b), and the results from both fractionation methods were compared to validate the complete particle dispersion in the fractionation procedure without SOM destruction (data not shown).

The non-fractionated soil (i.e., an aliquot of the 2 mm sieved, air-dried sample) and all fractions were then oven-dried at 40 °C, weighed, finely ground (< 200 μm) and analysed for C content based on the principle of the "Dumas method", which involves the complete and instantaneous oxidation of the sample by dry flash combustion using an elemental analyser (Carlo Erba, ThermoFlash or Fison instruments depending on the set). The soil samples collected in the study areas were expected to be carbonate free; thus, all the carbon was considered organic. For the fractions, C analysis yielded concentrations (gC kg^{-1} fraction); then, the C amount in each fraction (gC fraction kg^{-1} soil) was calculated as the product of the fraction C concentration and the fraction mass (g fraction kg^{-1} soil). For the non-fractionated soil, the C amount corresponds to the C concentration (both expressed in gC kg^{-1} soil); thus, for the sake of simplification, the term "C amount" will be preferentially used thereafter.

In the present study, for each sample, all fractions > 200 μm and 50–200 μm (heavy fraction and POM when they had been separated) were grouped together and referred to as F>50. This choice was based on preliminary tests that showed poorer predictions for these fractions separated than grouped (suggesting that they were not well differentiated; data not shown); this was consistent with Poeplau et al. (2018), who found no age difference between organic fractions > 200 μm and 50–200 μm. Thus, the variables of interest were the C amounts in the non-fractionated soil, F>50, F20-50 and F<20.

Precision in the determination of reference values has been recognized as a critical element for consideration in the NIRS model calibration and/or when assessing NIRS model accuracy (Coates, 2002; Yao et al., 2010). The standard error of laboratory, which is used to assess the precision of the reference method, can be calculated as follows (Workman, 2007):

$$SEL = \sqrt{\frac{\sum_{j=1}^{m}\sum_{i=1}^{n}(x_{ij} - \bar{x}_j)^2}{m \times (n-1)}} \quad (1)$$

where SEL is the standard error of laboratory; x_{ij} stands for the C amount in the considered fraction for each replicate i of each sample j; $\bar{x}_j$ is the C amount in the same fraction averaged over the replicates of sample j; n is the number of replicates per sample; and m is the number of samples.

For the target set, most fractionations were performed by one operator and the few others by two other operators, without replication in general. However, three of these samples were fractionated three times, and each replication was performed by a different operator; this enabled the estimation of the intermediate precision of the fractionation procedure (SEL_{int}; calculated from replicates on a given sample performed by different operators in a single laboratory; Ermer et al., 2005). The latter was considered the standard error of laboratory for the C amount in each fraction in the target sample set; in this case, Eq. (1) was used with n = 3 and m = 3. For the SSL subsets, fractionation was performed with two replicates per sample: on each of the four southern Benin samples, by one operator; on two of the five Togo samples, by another operator; to note, these operators were not involved in the fractionation of the target samples. These replications enabled the estimation of the repeatability of the fractionation procedure per sample subset (SEL_{repet}; calculated from replicates on a given sample performed by a single operator under the same conditions over a short interval of time; Sørensen, 2002; Ermer et al., 2005); this was calculated for the C amount in each fraction. For the southern Benin subset, Eq. (1) was used with n = 2 and m = 4, and for the Togo subset, with n = 2 and m = 2.

For C in the non-fractionated soil (i.e., SOC content), the SEL_{int} was not determined; however, considering the soil C range, SEL_{int} was estimated to be approximately 1 gC kg^{-1}. Indeed, Brown et al. (2005) reported a laboratory error of 1.1 gC kg^{-1} for the SOC content by replicating 12 samples selected from a sample set from north-central Montana (USA) with an average SOC content close to that of the validation set in the present study (7.2 gC kg^{-1} vs. 7.6 gC kg^{-1}); however, no details were provided on the number of operators, the time lapse between replications or the number of replications per sample. Stevens et al. (2013) also estimated SEL_{int} by duplication of C analyses on 22 samples obtained at the European scale and found 2.0 gC kg^{-1} (for a higher average SOC content in the total set, i.e., 29 gC kg^{-1}).

To evaluate the linear correlations between the studied variables (i.e., the C amounts in the non-fractionated soil, F<20, F20-50, and F>50), a matrix of Pearson's correlation coefficients was calculated for the entire sample set using the R package *PerformanceAnalytics* (*chart.Correlation* function; Peterson and Carl, 2020).

2.4. Spectrum acquisition

For all the sample sets, the same spectrum acquisition procedure was followed with the same instrument, but the acquisitions were performed during different periods (2008–2019) by different operators. Soil reflectance was measured under laboratory conditions on two aliquots of 2-mm sieved, air-dried soil samples, which were oven-dried overnight at 40 °C just before spectrum acquisition. Aliquots of approximately 5 g were placed in a ring cup and scanned in the NIR region between 1100 nm and 2498 nm every 2 nm (700 data points) using a Foss NIRSystems 5000 spectrophotometer (Laurel, MD, USA). The spectra were then averaged per sample and converted into absorbance [1/$\log_{10}$(reflectance)].

2.5. Pretreatments

The spectrum pretreatments tested and retained by Cambou et al. (2022) for sandy Senegalese soil samples were used to amplify the useful parts of spectra and reduce irrelevant information (by reducing baseline variations, enhancing spectral features, reducing the particle size scattering effect, removing linear or curvilinear trends of each spectrum, and/or removing additive or multiplicative signal effects): Savitzky-Golay smoothing (*Smoo*), centring (*Centr*), standard normal variate (*SNV*), 1st- and 2nd-order detrendings (*D1*, *D2*), 1st- and 2nd-order derivatives with 11- or 31-point gap (*Der111*, *Der131*, *Der211* and *Der231*); *SNV* followed by *D1* (*SNVD1*), *D2* (*SNVD2*) or the 1st- or 2nd-order derivatives mentioned (e.g., *SNVDer111*); *D1* or *D2* followed by the 1st-order derivatives mentioned (e.g., *D1Der111*); *SNVD1* or *SNVD2* followed by the 1st-order derivatives mentioned (e.g., *SNVD1Der111*). The raw absorbance spectra, with no pretreatment, were also studied (*Raw*). In total, 24 spectrum types were studied, including (i) 23 types of pretreated spectra and (ii) raw absorbance spectra. For simplicity, these spectrum types are referred to as spectral pretreatments. The spectral pretreatments were performed using the R packages *rchemo* (*savgol*, *snv*,

and *detrend* functions; Brandolini-Bunlon et al., 2023) and *prospectr* (*gapDer* function; Stevens and Ramirez-Lopez, 2022).

Since the distributions of the C amount in the non-fractionated soil and in the fractions were skewed (see Section 3.1), the decimal logarithmic transformation ($\log_{10}$) of these variables was carried out to achieve more normal distributions and was used for modelling to improve the prediction accuracy; then, the predictions ($\log_{10}$C) were back-transformed into C amounts (gC kg^{-1} soil; Cambou et al., 2022).

2.6. Selection of the calibration and validation sets

The replicated SSL samples (four from southern Benin and two from Togo; Section 2.3) were averaged for model calibration; thus, the SSL included 185 samples with data on C amount in the fractions and 184 samples with data on C amount in the non-fractionated soil (missing value for one sample in Congo-Brazzaville). However, four samples were then removed because they were considered outliers according to the C amount in the non-fractionated soil (> 39 gC kg^{-1} for these four samples; the average C amount in the non-fractionated soil in the SSL decreased from 8.4 to 7.7 gC kg^{-1} soil after outlier removal). Among these samples, three originated from southeastern Benin, and one from Togo. After outlier removal, the SSL included 181 samples with fractionation data and 180 samples with C amount in the non-fractionated soil; these samples were used for calibration.

Out of the 94 samples in the target set, 10 or 15 samples were not used for validation but were kept for spiking; specifically, they were used to enrich the calibration set. The 10 and 15 spiking samples were selected according to their spectral representativeness within the target set. For that purpose, a principal component analysis (PCA) was performed on the *Centr* spectra of the target set using the R package *FactoMineR* (*PCA* function; Lê et al., 2008). PCA condenses a large and redundant amount of information carried by spectra (here, absorbance at 700 wavelengths) into a small number of latent variables (LVs). The LVs are linear combinations of absorbances built to be orthogonal with each other (no redundancy) and to explain maximum variance (to represent at best spectral variability). Then, the Kennard-Stone algorithm (Kennard and Stone, 1969) was applied to PCA scores (i.e., sample coordinates on LVs) on the first three LVs (99.8% of the total variance) to select 15 spectrally representative samples using the R package *prospectr* (*kenStone* function; Stevens and Ramirez-Lopez, 2022) for spiking, and the remaining samples were used for validation (validation set; 79 samples). The second spiking subset, with 10 samples, was subsequently selected also using the Kennard-Stone algorithm applied to the same PCA scores, while ensuring that it was part of the initially selected subset of the 15 samples; then, the five remaining samples were removed and not considered such that the validation set was the same regardless of the spiking subset used. Finally, both spiking subsets (15 and 10 samples) were extra-weighted six times. This process resulted in 90 and 60 spiking samples, respectively, before addition to the SSL: these two subsets represented one-third and one-fourth of the final calibration set, respectively, which was assumed to be a sufficient proportion in the present study; to note, the spiking samples needed to carry just enough weight to avoid being overrepresented. The search for the optimal extra-weight was not the focus of this study, as this topic has been studied by other authors (Guerrero et al., 2014 for SOC content; Barthès et al., 2020 for SOC and SIC contents).

To assess both the benefits of using the SSL and of adding spiking with extra-weighting for calibrations, prediction models were separately built from five calibration sets: (i) SSL only (SSL; 180–181 samples); (ii) SSL with 15 spiking samples extra-weighted six times (SSL+6×15; 270–271 samples); (iii) SSL with 10 spiking samples extra-weighted six times (SSL+6×10; 240–241 samples); (iv) only the subset of 15 target samples selected for spiking (15-target); and (v) only the subset of 10 target samples selected for spiking (10-target). As mentioned previously, the validation set was constant and included 79 samples.

2.7. Regression procedures

Two partial least squares regression (PLSR) procedures were carried out: global PLSR and locally weighted PLSR.

The PLSR condenses the information carried by spectra into a small number of LVs that are both linear combinations of absorbances and orthogonal with each other, similar to PCA but also built to maximize their covariance with the response variable (e.g., the C amount in the non-fractionated soil). Then, regression is carried out with LVs as explanatory variables. Global PLSR is the common PLSR procedure: one prediction model is built using all calibration samples and is subsequently applied to all validation samples (Wold et al., 1983). Locally weighted PLSR (hereinafter called local PLSR) builds one prediction model for each validation sample individually and weights the contribution of all calibration samples to model building based on their spectral distance (or spectral similarity) from that validation sample (Boysworth and Booksh, 2008). The spectral distance was the Mahalanobis distance between the validation and calibration samples in a space of 10 PLS-LVs (number of PLS-LVs fixed arbitrarily) built on the calibration set. The weights assigned to the calibration samples to predict the validation sample considered were then calculated according to Brandolini-Bunlon et al. (2023) using Eq. (2):

$$w = e^{\left(\frac{-d}{h \times MAD(d)}\right)} \quad (2)$$

where w is the weight assigned to one calibration sample according to d, which is the Mahalanobis distance between this calibration spectrum and the validation spectrum considered; MAD(d) is the mean absolute deviation of the d values of the entire calibration dataset for the validation sample considered; and h is a positive scalar defining the shape of w (here, h = 1).

When the Mahalanobis distance between a calibration spectrum and the validation spectrum considered was greater than median(d) + 5 × MAD(d), the weight assigned to this calibration sample was set to zero.

Finally, the weights were standardized between 0 and 1 using Eq. (3):

$$w_{norm} = \frac{w}{\max(w)} \quad (3)$$

As a result, for each log-transformed variable (the C amount in the non-fractionated soil, F<20, F20-50, and F>50), two regression procedures (global and local) were performed using five calibration sets (SSL, SSL+6×15, SSL+6×10, 15-target, 10-target) with 24 spectral pretreatments. In each case, a randomly selected fivefold cross-validation (CV) with 10 replicates was performed on the calibration set, except for both target sets where the leave-one-out CV was performed due to their small size. Based on the CV results, the optimal number of LVs was selected between 3 and 15 according to the three following methods. In the first and most parsimonious method, a precision gain ratio (Rg) was calculated according to Eq. (4) (Brandolini-Bunlon et al., 2023):

$$\mathrm{Rg} = 1 - \frac{\mathrm{RMSECV}_{\mathrm{NLV}+1}}{\mathrm{RMSECV}_{\mathrm{NLV}}} \quad (4)$$

where Rg is the relative gain in efficiency after a new LV was added to the model and RMSECV is the root mean square error of cross-validation for the two successive numbers of LVs (NLV and NLV+1). In the present study, the iterations stopped when Rg became lower than a threshold value, which was set at 2% after the preliminary tests, and the corresponding NLV was considered optimal. In the second and least parsimonious method, the selected number of LVs was the one that minimized the RMSECV (NLVmin). In the third and intermediate method, the precision loss ratio (Rl) was calculated according to Eq. (5):

$$\mathrm{Rl} = \frac{\mathrm{RMSECV}_{\mathrm{NLVmin-i}} - \mathrm{RMSECV}_{\mathrm{NLVmin}}}{\mathrm{RMSECV}_{\mathrm{NLVmin}}} \quad (5)$$

where Rl is the relative loss in efficiency after removing i LVs from NLVmin, which minimizes the RMSECV. The selected number of LVs was the lowest when Rl was lower than a certain threshold value, which was set at 5% after preliminary tests.

Finally, when a prediction yielded a negative value, it was replaced by zero.

All regression procedures were performed using the R package *rchemo* (*segmkf*, *gridcvlv*, *selwold*, *plskern*, *predict.Plsr*, *lwplsr*, and *predict.Lwplsr* functions; Brandolini-Bunlon et al., 2023).

2.8. Evaluation of model accuracy

Model accuracy was evaluated on back-transformed predictions (the C amounts in units of gC kg^{-1} soil since the predictions were performed on log-transformed data).

The first parameter used for assessing the prediction accuracy was the root mean square error of the prediction over the validation set (RMSEP). RMSEP actually includes the laboratory uncertainty (SEL_{int} in the present study) as follows (Fernández-Ahumada et al., 2006):

$$RMSEP^2 = SEL_{int}{}^2 + RMSEP_{nir}^2 \quad (6)$$

where $RMSEP_{nir}$ is the root mean square error of prediction only due to prediction using NIR spectra. However, the number of samples on which replications had been carried out was too small to allow a proper estimation of SEL_{int}.

Additional parameters were also considered to evaluate model accuracy:

- the bias, which is the mean residue over the validation set;
- the coefficient of determination (i.e., the squared correlation coefficient; R^2) between the predictions and observations calculated over the validation set (R^2_{VAL});
- the ratio of performance to the interquartile range in the validation set ($RPIQ_{VAL}$), which is the ratio of the interquartile range (i.e., difference between the third and first quartiles; IQR) over the validation set to the RMSEP. This ratio has been recommended instead of the ratio of performance to the deviation (RPD_{VAL}, which is the ratio of the standard deviation, SD, calculated over the validation set to the RMSEP) for variables that do not follow a normal distribution (Bellon-Maurel et al., 2010). In the present study, the log-transformed variables did not systematically follow a normal distribution; thus, $RPIQ_{VAL}$ was preferred to RPD_{VAL} for interpreting model accuracy. The threshold proposed by Ludwig et al. (2018) was used, and a successful (or accurate) prediction was defined by $RPIQ_{VAL} \geq 1.9$.

3. Results

3.1. Conventional analyses

When referring to the C amount in the non-fractionated samples, the C recovery after fractionation averaged 91% across all samples; however, there were differences between sets: 88% and 99% for Burkina Faso (two sets), 92% for the Congo, 101% for Togo, 96% for Cameroon, 84% for southern Benin, 78% for southeastern Benin, and 90% for the target set.

Table 2 and Fig. S1 (Supplementary Material) show the distribution statistics of the C amount in the non-fractionated soil and in F<20, F20-50 and F>50 for the SSL, 10-target, 15-target, and validation set. The distributions of the C amount in the non-fractionated soil and in the different fractions followed the same trend; the distributions were quite similar between the validation set and the 10-target subset but tended to include higher values in the 15-target subset and were wider in the SSL. The distribution of each response variable in the validation set was generally included or close to the distribution of this variable in the calibration sets. Most distributions were markedly asymmetric, which was the reason for using log-transformed values of the C amounts (log_{10}) for modelling.

The largest C amounts were found in F<20 (40–50% on average) and F>50 (30–40%), while F20-50 had much less C (ca. 10%). The C amount in each fraction was closely correlated with the C amount in the non-fractionated soil (Pearson's correlation coefficient = 0.82–0.93) and, to a lesser extent, with the C amounts in the other fractions (Pearson's correlation coefficient = 0.72–0.74; Fig. 2).

The study of the effects of land use and management on the C distribution in particle size and/or density fractions (e.g., more POM under forest than under permanent cropping) was not the topic of the present study, as it has already been studied by many authors (Feller and Beare, 1997; Balesdent et al., 1998; d'Annunzio et al., 2008; Ramesh et al., 2019).

3.2. Spectra

Fig. 3 shows the space of the two first dimensions (Dim1, Dim2) of

Table 2
Distribution of C amount (gC kg^{-1} soil) in the non-fractionated soil and in the studied particle size fractions 0–20 μm (F<20), 20–50 μm (F20-50), and 50–2000 μm (F>50) in the soil spectral library (SSL), both sets used for spiking (15-target and 10-target) and the validation set. N is the number of samples, SD the standard deviation, IQR the interquartile range (difference between third and first quartiles) and Skew the skewness (unitless).

Fraction	Set	N	Median	IQR	Mean	SD	Min	Max	Skew
Non-fractionated soil (<2 mm)	SSL	180	7.3	7.7	9.7	7.1	1.6	36.0	1.5
	15-target	15	7.5	11.4	11.1	7.8	2.3	28.2	0.8
	10-target	10	6.2	4.1	7.8	5.6	2.3	23.3	1.7
	Validation	79	6.6	4.9	7.6	4.0	2.4	23.9	1.5
F<20	SSL	181	3.2	2.6	4.1	2.6	1.1	14.3	1.4
	15-target	15	4.4	4.1	4.9	3.0	1.1	11.9	0.8
	10-target	10	3.1	2.4	3.7	2.0	1.1	8.3	0.8
	Validation	79	3.0	2.1	3.4	1.6	1.3	10.3	1.6
F20-50	SSL	181	0.5	0.7	0.7	0.7	0.1	3.4	1.6
	15-target	15	0.8	1.1	1.0	0.8	0.2	2.9	0.8
	10-target	10	0.5	0.5	0.7	0.8	0.2	2.9	1.8
	Validation	79	0.6	0.6	0.8	0.5	0.1	2.1	1.0
F>50	SSL	181	2.5	3.6	3.9	3.7	0.3	21.6	1.9
	15-target	15	1.6	5.2	4.0	3.9	0.5	13.3	1.0
	10-target	10	1.3	0.8	2.4	2.7	0.5	10.0	1.9
	Validation	79	1.9	2.3	2.6	1.9	0.5	11.0	1.7

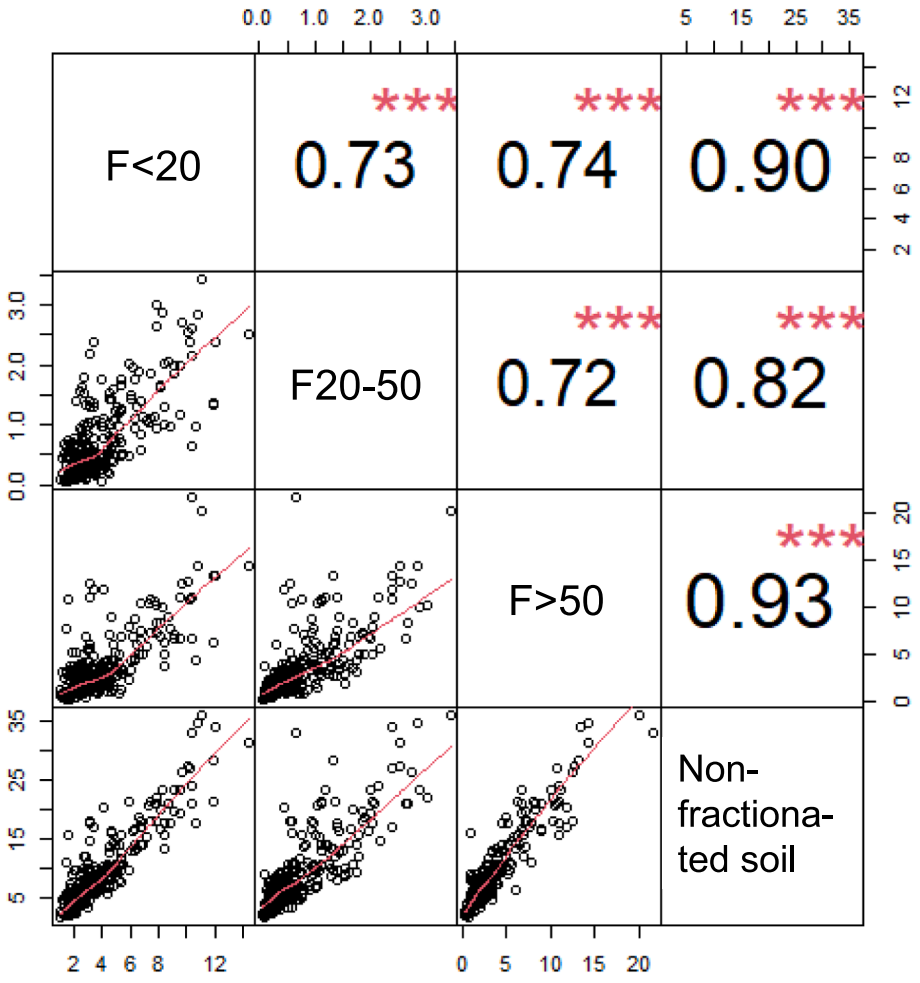

Fig. 2. Matrix of Pearson's correlation coefficients (on the top of the diagonal) and bivariate scatter plots with fitted lines (on the bottom of the diagonal) between the observed C amounts (gC kg^{-1} soil) in the non-fractionated soil, F<20, F20-50, and F>50 for the whole dataset (274 samples). The symbol "***" is associated to a significant correlation with a p-value < 0.001.

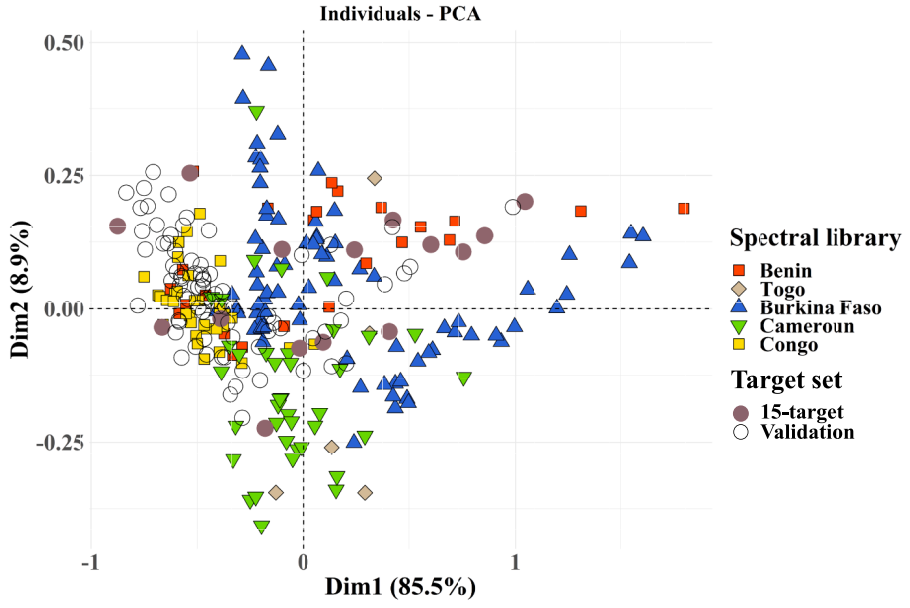

Fig. 3. Projection of the studied soil samples, grouped by countries, on the two first components of the PCA built on smoothed then centred NIR spectra of the soil spectral library, where the target samples (15-target selected for spiking and the validation set) were then added as supplementary individuals.

Table 3
Validation results for NIRS predictions of C amount in the non-fractionated soil (gC kg^{-1}) for each PLSR method, which was calibrated on (i) the soil spectral library (SSL) alone, (ii) SSL with spiking sets extra-weighted six times, or (iii) the target sets used for spiking alone (15-target and 10-target). For each parameter, the left-hand number was obtained with the spectral pretreatment that minimized RMSEP (i.e. raw or pretreated spectra, specified in table footnotes); the right-hand number is the value averaged over the 24 spectral pretreatments (with the standard deviation, SD). The mean ± SD of C amount in non-fractionated soil was 7.6 ± 4.0 gC kg^{-1} in the validation set. The RMSEP and bias are expressed in gC kg^{-1}; the other parameters are unitless.

CAL set	N_{CAL}	N LV	R^2_{VAL}	Bias	RMSEP	$RPIQ_{VAL}$
Global PLSR						
SSL[a]	180	7; 9 (2)	0.71; 0.71 (0.03)	1.3; 2.7 (0.7)	2.6; 3.6 (0.6)	1.8; 1.4 (0.2)
SSL+6×15[b]	270	8; 10 (2)	0.75; 0.72 (0.02)	0.4; 0.7 (0.3)	2.1; 2.3 (0.2)	2.4; 2.1 (0.1)
SSL+6×10[c]	240	9; 9 (1)	0.76; 0.73 (0.02)	0.3; 0.7 (0.3)	2.0; 2.4 (0.3)	2.4; 2.1 (0.2)
15-target[d]	15	3; 3 (1)	0.73; 0.71 (0.02)	0.0; −0.2 (0.1)	2.1; 2.2 (0.1)	2.3; 2.2 (0.1)
10-target[e]	10	3; 3 (1)	0.75; 0.70 (0.03)	−0.1; −0.2 (0.2)	2.0; 2.3 (0.1)	2.4; 2.2 (0.1)
Local PLSR						
SSL[f]	180	6; 8 (2)	0.77; 0.71 (0.05)	2.3; 3.2 (0.6)	3.1; 4.2 (0.7)	1.6; 1.2 (0.2)
SSL+6×15[c]	270	3; 7 (2)	0.77; 0.73 (0.04)	0.1; 0.7 (0.3)	1.9; 2.4 (0.3)	2.5; 2.1 (0.3)
SSL+6×10[c]	240	4; 7 (2)	0.77; 0.73 (0.04)	0.4; 0.7 (0.3)	2.0; 2.5 (0.4)	2.5; 2.0 (0.3)
15-target[f]	15	3; 3 (1)	0.80; 0.73 (0.07)	0.2; 0.2 (0.4)	1.8; 2.3 (0.6)	2.7; 2.2 (0.4)
10-target[g]	10	3; 3 (1)	0.82; 0.73 (0.06)	0.0; −0.1 (0.1)	1.8; 2.1 (0.2)	2.8; 2.3 (0.3)

[a]*SNV*; [b]*SNVDer111*; [c]*SNVD1Der131*; [d]*D1Der111*; [e]*Der211*; [f]*Der131*; [g]*SNVD1Der111*.

the PCA built using the *Centr* spectra of the SSL, where the *Centr* spectra of the target set were then projected. A noticeable proportion of the target spectra were outside the area circumscribed by the SSL samples in the PCA plane, which indicated that they were not effectively represented by the SSL in this space, and justified spiking. In the PCA plane considered, however, some SSL samples from the Congo, Cameroon and southeastern Benin were close to the validation samples.

3.3. Predictions of the C amounts in the non-fractionated soil and fractions

Briefly, the global PLSR builds one prediction model using all calibration samples, which is subsequently applied to all validation samples, while the local PLSR builds one prediction model for each validation sample individually by weighting the contribution of calibration samples based on their spectral similarity to that validation sample.

In the preliminary step, when the SSL was used for calibration, the RMSEP was almost always lower when the number of LVs was optimized with the most parsimonious method than when the other methods were used (data not shown). Thus, only the results obtained with the most parsimonious method are reported hereafter.

For each fraction, the PLSR procedure and calibration set considered, the text of this section will focus on the results achieved with the spectrum pretreatment (i.e., raw or pretreated) that yielded the lowest RMSEP; additionally, the tables also provide the average results (with SDs) achieved over the 24 spectral pretreatments tested.

3.3.1. Prediction of the C amount in the non-fractionated soil

Table 3 provides the validation results for the C amount in the non-fractionated soil. The most accurate model was obtained with local calibration on 10-target: the RMSEP was 1.8 gC kg^{-1}, and the corresponding $RPIQ_{VAL}$ and R^2_{VAL} were 2.8 and 0.82, respectively. The predictions were comparable when using 15-target or SSL spiked in both local and global PLSR (lowest RMSEP = 1.8–2.1 gC kg^{-1}). The predictions were much poorer when using SSL alone (lowest RMSEP = 2.6–3.1 gC kg^{-1}), due to a particularly large bias, especially in local calibration; moreover, the result was less stable over the spectral pretreatments (SD of RMSEP was 0.6–0.7 gC kg^{-1} when using SSL alone vs. 0.2–0.4 gC kg^{-1} when SSL was spiked). Except for the SSL alone, local calibration tended to provide better predictions than global calibration when using the most appropriate spectral pretreatments; to note, this was not clear for the average over all spectral pretreatments.

Fig. 4 shows the comparisons between the measured C amounts and the predicted C amounts in the non-fractionated soil and in the fractions for the validation set using the models built with different calibration sets. Specifically, it shows for each variable and calibration set, the PLSR model (global or local) and spectral pretreatment, which minimized RMSEP. With regard to the non-fractionated soil, Fig. 4a highlights that predictions were biased when using SSL alone, especially at low C values (< 8 gC kg^{-1}) and that spiking both reduced the bias and improved the predictions for the highest C values (> 20 gC kg^{-1}).

3.3.2. Prediction of the C amount in F<20

Table 4 presents the validation results for the C amount in F<20. The most accurate predictions were achieved with global PLSR on SSL+6×15 and local PLSR on SSL+6×10 (the lowest RMSEP was 0.9 gC kg^{-1} soil, and the corresponding $RPIQ_{VAL}$ and R^2_{VAL} were 2.3 and 0.68, respectively). However, the global PLSR on SSL+6×10 and the local PLSR on SSL+6×15 yielded nearly identical results. The prediction accuracy tended to be slightly lower when using 10-target or 15-target only (lowest RMSEP = 0.9–1.0 gC kg^{-1} soil) but was clearly lower when using SSL alone (lowest RMSEP = 1.2–1.3 gC kg^{-1} soil), with noticeable bias in both cases (negative for target samples only, positive for SSL alone, and negligible when using both). Moreover, over the five calibration sets considered, the prediction accuracy was nearly identical for the global and local calibration. Fig. 4b shows that using SSL+6×10 improved the prediction for all validation samples compared to using SSL alone.

3.3.3. Prediction of the C amount in F20-50

Table 5 presents the validation results for C in F20-50. The most accurate model was achieved with local PLSR on SSL+6×15 (the lowest RMSEP was 0.3 gC kg^{-1} soil, and the corresponding $RPIQ_{VAL}$ and R^2_{VAL} were 2.0 and 0.60, respectively). However, differences according to the regression procedure (global or local), calibration set (with or without SSL or spiking) and/or spectral pretreatment were limited (e.g., the lowest RMSEP was always 0.3 gC kg^{-1} soil), which is highlighted in Fig. 4c.

3.3.4. Prediction of the C amount in F>50

Table 6 presents the validation results for the C amount in F>50. The most accurate model was achieved with local PLSR calibrated on SSL+6×10; the lowest RMSEP was 1.0 gC kg^{-1} soil, and the corresponding $RPIQ_{VAL}$ and R^2_{VAL} were 2.3 and 0.73, respectively. However, comparable predictions were achieved with the global calibration using SSL+6×15 with the same lowest RMSEP, bias and $RPIQ_{VAL}$; however, a

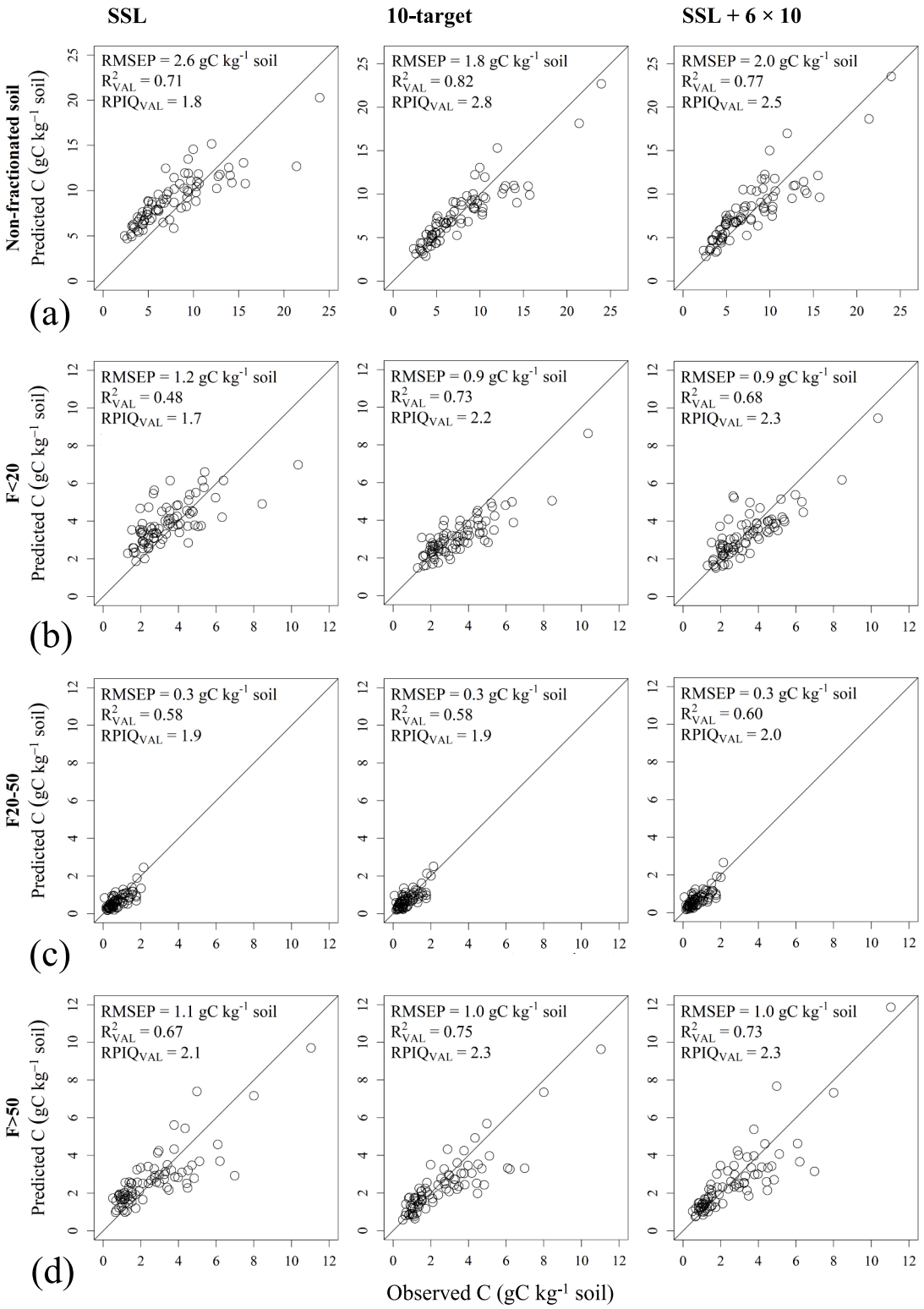

Fig. 4. Observed vs. predicted C amounts (gC kg^{-1} soil) in (a) the non-fractionated soil, and the particle size fractions (b) 0–20 μm (F<20), (c) 20–50 μm (F20-50), and (d) 50–2000 μm (F>50), for the validation set, using three calibration datasets: (i) the spectral library alone (SSL), (ii) the 10-target alone, and (iii) SSL with 10 spiking samples extra-weighted six times (SSL+6×10). In each case, the model shown was obtained with the spectral pretreatment (i.e. raw or pretreated) and the PLSR method that minimized RMSEP (global PLSR for the non-fractionated soil, local PLSR for the fractions). The line represents $y = x$.

slight loss in the prediction accuracy was observed when considering the average results over the 24 pretreatments. Additionally, comparable predictions were obtained with local calibration using SSL+6×15 (lowest RMSEP = 1.0 gC kg^{-1} soil). Compared with the calibration on SSL spiked, the calibration on 10-target, 15-target or SSL alone could cause a slight decrease in prediction accuracy. This was slightly noticeable with local calibration (lowest RMSEP = 1.0–1.1 gC kg^{-1} soil) but more noticeable with global calibration (lowest RMSEP = 1.2 gC kg^{-1} soil); these both were caused by a larger bias. In the local calibration, compared with the calibration on SSL spiked, the calibration

Table 4
Validation results for NIRS predictions of C amount in F<20 (gC kg^{-1} soil) for each PLSR method, which was calibrated on (i) the soil spectral library (SSL) alone, (ii) SSL with spiking sets extra-weighted six times, or (iii) the target sets used for spiking alone (15-target and 10-target). For each parameter, the left-hand number was obtained using the spectral pretreatment that minimized RMSEP (i.e. raw or pretreated spectra, specified in table footnotes); the right-hand number is the value averaged over the 24 spectral pretreatments (with the standard deviation, SD). The mean ± SD of C amount in F<20 was 3.4 ± 1.6 gC kg^{-1} soil in the validation set. The RMSEP and bias are expressed in gC kg^{-1} soil; the other parameters are unitless.

CAL set	N_{CAL}	N LV	R^2_{VAL}	Bias	RMSEP	$RPIQ_{VAL}$
Global PLSR						
SSL[a]	181	6; 10 (2)	0.49; 0.41 (0.08)	0.6; 0.8 (0.1)	1.3; 1.5 (0.1)	1.6; 1.4 (0.1)
SSL+6×15[b]	271	11; 11 (2)	0.68; 0.63 (0.03)	0.1; 0.0 (0.1)	0.9; 1.0 (0.0)	2.3; 2.1 (0.1)
SSL+6×10[c]	241	15; 11 (2)	0.67; 0.63 (0.02)	0.1; 0.1 (0.1)	0.9; 1.0 (0.0)	2.3; 2.1 (0.1)
15-target[d]	15	4; 4 (1)	0.69; 0.52 (0.11)	−0.3; −0.3 (0.1)	1.0; 1.2 (0.2)	2.2; 1.8 (0.3)
10-target[e]	10	4; 4 (1)	0.73; 0.63 (0.07)	−0.3; −0.4 (0.0)	0.9; 1.0 (0.1)	2.2; 2.0 (0.1)
Local PLSR						
SSL[d]	181	3; 8 (2)	0.48; 0.44 (0.05)	0.5; 1.0 (0.2)	1.2; 1.6 (0.2)	1.7; 1.3 (0.1)
SSL+6×15[f]	271	9; 7 (2)	0.66; 0.60 (0.04)	−0.1; 0.0 (0.1)	0.9; 1.0 (0.1)	2.2; 2.0 (0.1)
SSL+6×10[f]	241	9; 8 (2)	0.68; 0.60 (0.05)	−0.1; 0.0 (0.1)	0.9; 1.0 (0.1)	2.3; 2.0 (0.2)
15-target[g]	15	3; 4 (1)	0.74; 0.54 (0.10)	−0.5; −0.3 (0.1)	1.0; 1.2 (0.2)	2.2; 1.8 (0.3)
10-target[e]	10	4; 4 (1)	0.70; 0.64 (0.04)	−0.3; −0.3 (0.0)	0.9; 1.0 (0.1)	2.2; 2.1 (0.1)

[a]*SNVDer131*; [b]*Centr*; [c]*D2Der131*; [d]*Raw*; [e]*SNVDer211*; [f]*SNVDer111*; [g]*Smoo*.

on SSL, 10-target or 15-target alone affected the variability of the RMSEP depending on the spectral pretreatment; the SDs of the RMSEP were 0.2–0.4 for SSL, 10-target or 15-target alone vs. 0.1 gC kg^{-1} soil for SSL spiked.

When spiking samples were added to SSL, the global and local models yielded nearly identical accuracies; however, the prediction accuracy for SSL, 10-target or 15-target alone was slightly better when using the local calibration rather than the global calibration. Fig. 4d shows that adding spiking samples to the SSL improved the predictions of the lowest C values (< 2 gC kg^{-1} soil) compared to the predictions with the SSL alone.

3.3.5. Prediction accuracy for all variables

The benefit of spiking (with extra-weighting) was large for the C amount in the non-fractionated soil (the best models did not even use the SSL), noticeable for the C amount in F<20, limited for the C amount in F>50 and negligible for the C amount in F20-50. The optimal number of spiking samples (15 vs. 10) added to the SSL depended on the studied variable and the regression procedure. No clear trend could be drawn, except that prediction accuracy tended to be more affected by the spectral pretreatment with 10 than with 15 spiking samples; specifically, the SD of RMSEP over 24 spectral pretreatments tended to be higher with 10 than 15 spiking samples. The benefit of adding the SSL to the target samples for predicting C amounts was generally lower, and even nil for C in the non-fractionated soil. Moreover, when compared to the global calibration, the local calibration generally had a limited benefit and was even detrimental in some cases (e.g., when using SSL alone for predicting the C amount in the non-fractionated soil).

The comparison of model accuracies between the variables when considering $RPIQ_{VAL}$ showed that the best predictions of the C amount were achieved for the non-fractionated soil (highest $RPIQ_{VAL} = 2.8$) and the worst for F20-50 (highest $RPIQ_{VAL} = 2.0$), with intermediate results for F<20 and F>50 (highest $RPIQ_{VAL} = 2.3$ in both cases). These results were achieved with SSL spiked, except for C in the non-fractionated soil (target samples alone), and in local calibration, except for F<20. When the SSL was used alone, the model accuracy was the highest for F>50 (local calibration; $RPIQ_{VAL} = 2.1$), followed by F20-50 (global or local calibration; $RPIQ_{VAL} = 1.9$), the non-fractionated soil (global

Table 5
Validation results for NIRS predictions of C amount in F20-50 (gC kg^{-1} soil) for each PLSR method, which was calibrated on (i) the soil spectral library (SSL) alone, (ii) SSL with spiking sets extra-weighted six times, or (iii) the target sets used for spiking alone (15-target and 10-target). For each parameter, the left-hand number was obtained using the spectral pretreatment that minimized RMSEP (i.e. raw or pretreated spectra, specified in table footnotes); the right-hand number is the value averaged over the 24 spectral pretreatments (with the standard deviation, SD). The mean ± SD of C amount in F20-50 was 0.8 ± 0.5 gC kg^{-1} soil in the validation set. The RMSEP and bias are expressed in gC kg^{-1} soil; the other parameters are unitless.

CAL set	N_{CAL}	N LV	R^2_{VAL}	Bias	RMSEP	$RPIQ_{VAL}$
Global PLSR						
SSL[a]	181	6; 8 (2)	0.57; 0.46 (0.05)	0.1; −0.1 (0.1)	0.3; 0.4 (0.0)	1.9; 1.6 (0.2)
SSL+6×15[b]	271	9; 11 (2)	0.57; 0.52 (0.04)	−0.1; 0.0 (0.0)	0.3; 0.3 (0.0)	1.9; 1.8 (0.1)
SSL+6×10[c]	241	5; 11 (3)	0.57; 0.52 (0.03)	−0.1; 0.0 (0.0)	0.3; 0.4 (0.0)	1.9; 1.7 (0.1)
15-target[d]	15	3; 4 (1)	0.56; 0.52 (0.03)	0.0; 0.0 (0.1)	0.3; 0.4 (0.1)	1.9; 1.7 (0.2)
10-target[e]	10	3; 3 (1)	0.52; 0.51 (0.02)	0.0; 0.0 (0.0)	0.3; 0.4 (0.0)	1.8; 1.7 (0.1)
Local PLSR						
SSL[f]	181	7; 6 (1)	0.58; 0.54 (0.03)	−0.1; −0.1 (0.1)	0.3; 0.4 (0.0)	1.9; 1.7 (0.1)
SSL+6×15[g]	271	6; 7 (2)	0.60; 0.57 (0.02)	0.0; 0.0 (0.0)	0.3; 0.3 (0.0)	2.0; 1.8 (0.1)
SSL+6×10[h]	241	5; 7 (2)	0.60; 0.55 (0.03)	−0.1; 0.0 (0.1)	0.3; 0.4 (0.0)	2.0; 1.6 (0.2)
15-target[i]	15	3; 4 (1)	0.56; 0.53 (0.05)	−0.1; 0.0 (0.1)	0.3; 0.4 (0.1)	1.9; 1.7 (0.3)
10-target[g]	10	3; 3 (1)	0.58; 0.53 (0.03)	0.0; 0.0 (0.0)	0.3; 0.4 (0.0)	1.9; 1.7 (0.1)

[a]*Der231*; [b]*Der111*; [c]*SNVDer231*; [d]*Der211*; [e]*SNVD1Der111*; [f]*SNV*; [g]*SNVD1Der111*; [h]*SNVD1*; [i]*SNVDer211*.

Table 6
Validation results for NIRS predictions of C amount in F>50 (gC kg^{-1} soil) for each PLSR method, which was calibrated on (i) the soil spectral library (SSL) alone, (ii) SSL with spiking sets extra-weighted six times, or (iii) the target sets used for spiking alone (15-target and 10-target). For each parameter, the left-hand number was obtained using the spectral pretreatment that minimized RMSEP (i.e. raw or pretreated spectra, specified in table footnotes); the right-hand number is the value averaged over the 24 spectral pretreatments (with the standard deviation, SD). The mean ± SD of C amount in F >50 was 2.6 ± 1.9 gC kg^{-1} soil in the validation set. The RMSEP and bias are expressed in gC kg^{-1} soil; the other parameters are unitless.

CAL set	N_{CAL}	N LV	R^2_{VAL}	Bias	RMSEP	$RPIQ_{VAL}$
Global PLSR						
SSL[a]	181	6; 7 (1)	0.61; 0.58 (0.04)	0.2; 0.6 (0.4)	1.2; 1.5 (0.2)	1.9; 1.6 (0.2)
SSL+6×15[b]	271	7; 8 (1)	0.71; 0.65 (0.03)	−0.1; 0.1 (0.1)	1.0; 1.2 (0.1)	2.3; 2.0 (0.2)
SSL+6×10[c]	241	8; 8 (2)	0.68; 0.63 (0.02)	−0.1; 0.0 (0.2)	1.1; 1.3 (0.1)	2.1; 1.8 (0.2)
15-target[d]	15	3; 4 (1)	0.65; 0.63 (0.02)	−0.3; −0.2 (0.2)	1.2; 1.4 (0.2)	2.0; 1.7 (0.2)
10-target[e]	10	3; 3 (1)	0.66; 0.60 (0.03)	−0.4; −0.4 (0.1)	1.2; 1.3 (0.1)	2.0; 1.8 (0.2)
Local PLSR						
SSL[f]	181	5; 5 (1)	0.67; 0.62 (0.06)	0.1; 0.4 (0.2)	1.1; 1.3 (0.2)	2.1; 1.8 (0.2)
SSL+6×15[f]	271	5; 5 (1)	0.71; 0.66 (0.02)	−0.1; −0.1 (0.1)	1.0; 1.2 (0.1)	2.2; 2.0 (0.1)
SSL+6×10[g]	241	6; 5 (1)	0.73; 0.67 (0.04)	−0.1; −0.1 (0.1)	1.0; 1.1 (0.1)	2.3; 2.0 (0.2)
15-target[e]	15	3; 3 (1)	0.74; 0.67 (0.04)	−0.4; 0.0 (0.3)	1.0; 1.3 (0.4)	2.2; 1.8 (0.4)
10-target[h]	10	3; 3 (1)	0.75; 0.63 (0.07)	−0.2; −0.2 (0.1)	1.0; 1.2 (0.2)	2.3; 1.9 (0.3)

[a]*SNVDer111*; [b]*SNV*; [c]*SNVDer231*; [d]*D2Der111*; [e]*SNVDer211*; [f]*SNVD1*; [g]*SNVDer131*; [h]*SNVD2Der111*.

calibration; $RPIQ_{VAL} = 1.8$) and F<20 (local calibration; $RPIQ_{VAL} = 1.7$).

Fig. 5 shows an example of regression coefficients obtained for each response variable by global PLSR calibrated on SSL+6×15, with *Centr* spectral pretreatment (the number of LVs was chosen using the most parsimonious method presented in Section 2.7). The regions that contributed most to the prediction of the C amounts in the non-fractionated soil and in all fractions were approximately 1380–1400 nm (positive then negative peaks for all variables), 1910–1930 nm (negative peaks for the non-fractionated soil and F<20; positive peaks for F20-50 and F>50), and 2225–2400 nm (positive then negative peaks for all variables). However, some regions strongly contributed to the prediction of the C amount in the fractions but not to the prediction of the C amount in the non-fractionated soil; these regions include the following: 1780–1850 nm (for F20-50 only), 1888–1896 nm (for the three fractions), and 2208–2210 nm (for F20-50 and F>50 only). In contrast, the regions that contributed strongly to the prediction of the C amount in the non-fractionated soil also contributed to the prediction of the C amount in at least one fraction.

3.4. Consideration of laboratory uncertainty

The SEL_{int} reached 0.6, 0.6 and 0.8 gC kg^{-1} soil for the three fractions F<20, F20-50 and F>50, respectively (Table S1; Supplementary Material), while the lowest RMSEP values for these fractions were 0.9, 0.3 and 1.0 gC kg^{-1} soil, respectively (Tables 4, 5 and 6). When performed by different operators, the fractionation procedure was thus a high source of variation that could affect the evaluation of prediction accuracy. In contrast, the SEL_{repet} values calculated for four replicated samples from southern Benin and two replicated samples from Togo were much lower. Specifically, the SEL_{repet} reached 0.1, < 0.1 and 0.2 gC kg^{-1} soil in both cases for the three fractions F<20, F20-50 and F>50, respectively.

4. Discussion

4.1. Ability of near-infrared spectroscopy to predict the C amount in the non-fractionated soil

When considering the RPIQ threshold proposed by Ludwig et al. (2018), SSL without spiking yielded inaccurate predictions of the C amount in the non-fractionated soil (i.e., SOC content) in the global and local calibrations. The difficulty in estimating SOC content at a local site using an independent SSL confirmed the results reported by Brown et al. (2005). In their study, the prediction of SOC content at one site using a model calibrated on five other sites in north central Montana (USA) yielded a RMSEP up to four times greater than that obtained when calibration and validation samples were randomly selected. Gogé et al. (2014) used a large VNIR SSL that represented the topsoils in France (2126 samples collected at 0–30 cm depth) to predict the SOC content in a 24-km^2 agricultural area in southern France. These authors obtained poorer results than in the present study (RPD_{VAL} was 0.6 with global PLSR and 1.2 with local PLSR vs. 1.5 and 1.3, respectively, in the present study, when using SSL alone; data not shown). However, they achieved much better predictions with local than with global calibration; this was opposite to the results from the present study, where global calibration was moderately more accurate than local calibration. In the present study, a high bias was observed for models calibrated on SSL alone. In addition to differences between the soils of the SSL and the validation set, differences in the conditions of spectral acquisition over time could also contribute to the biases observed (Shahbazikhah and Kalivas, 2013; Mark and Workman, 2017); indeed, spectral acquisitions were performed with the same spectrometer but by different operators between 2008 and 2019.

4.2. Prediction of fraction C amounts

The calibration based on SSL alone also yielded inaccurate predictions for the C amount in F<20 ($RPIQ_{VAL}$ = 1.7) but accurate predictions for the C amount in F20-50 and F>50 ($RPIQ_{VAL}$ = 1.9–2.1). To our knowledge, no study has reported predictions of SOC pools with such independent validation procedure. However, some studies have predicted SOC pools without independent validation. Barthès et al. (2008) used NIRS and global PLSR to predict the C amount in soil particle size fractions at three sites in Burkina Faso and at one site in Congo-Brazzaville (some samples were used in the SSL of the present study; Section 2.1). In their study, all samples were considered to belong to the same set, and the calibration and validation datasets were selected according to spectral representativeness, such as the method used in the present study to select the spiking samples. Indeed, the validation results achieved in the present study when using SSL spiked were comparable to those in their study for the C amounts in F<20 (R^2_{VAL} = 0.66–0.68 vs. 0.70, respectively) and F>50 (R^2_{VAL} = 0.68–0.73 vs. 0.65–0.78, respectively), and moderately less accurate than those in their study for the C amounts in F20-50 (R^2_{VAL} = 0.57–0.60 vs. 0.69, respectively). In the present study, the spiking samples represented a small proportion of the target set, while in Barthès et al. (2008), the calibration set represented

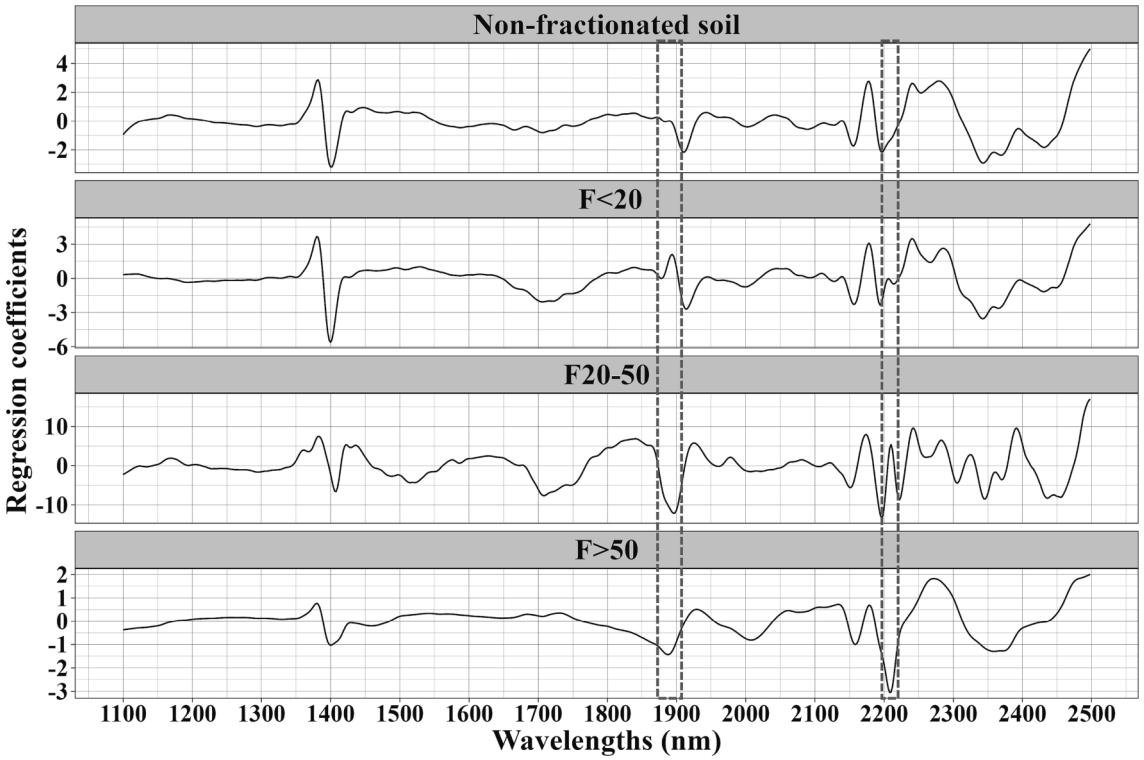

Fig. 5. Regression coefficients for the prediction of C amount in the non-fractionated soil, and in the three fractions (F<20, F20-50, F>50) calibrated with global PLSR on the centred spectra (*Centr*) using the dataset including the soil spectral library (SSL) with 15 spiking samples extra-weighted six times (SSL+6×15). The dotted rectangles highlight some examples of peaks present for at least two fractions but absent for the non-fractionated soil.

more than half of the total set, which could justify more accurate predictions in the latter case. However, the soil diversity in the target set of the present study (one small region) was lower than that in the total set of Barthès et al., (2008; one small region in the Congo and three sites in Burkina Faso) and could therefore be represented by a smaller number of samples. Yang et al. (2012) studied a set of clay loam soils on one Canadian farm and obtained excellent NIRS predictions for C amount in POM (> 50 μm; $R^2 = 0.92$); however, these results were achieved via leave-one-out cross-validation, which provides optimistic prediction results when several samples originate from the same site and soil profile (Brown et al., 2005); moreover, the sample soil diversity was limited (mineralogy, texture, land use, etc.). Ramifehiarivo et al. (2023) also used NIR spectra of non-fractionated soil to predict the C amount in particle size and density fractions for a set of 134 topsoil samples from Madagascar (seven sites, with one containing 56 samples). In their study, the calibration and validation sets (80% and 20%, respectively, which requires a great effort of fractionation) were selected according to spectral representativeness, and models were built using local PLSR. They reported better predictions for POM than in the present study for F>50 ($RPIQ_{VAL} = 3.4$ vs. 2.3, respectively). However, the greater accuracy of their models was particularly notable for F<20 ($RPIQ_{VAL} = 8.4$ vs. 2.2 in the present study). This result could be explained by the following: (i) the different strategies used for selecting calibration samples between the two studies, since in their case, all calibration samples were selected to be spectrally representative of the target set; (ii) the smaller proportion of samples used for validation in their study (20%, i.e., 25 samples); (iii) the high proportion of F<20 in the soils of their set and the large C amount it accounted for (on average 22 vs. 4 gC kg^{-1} soil in the present study, where soils were mostly coarse-textured); and (iv) fine sample grinding before NIRS acquisitions (< 0.2 mm vs. < 2 mm in the present study), which results in uniform SOM distribution in the sample, and therefore in the subsamples used for conventional and spectral measurements; that facilitates modelling (Barthès et al., 2006) but requires additional soil preparation. Other results are available in the literature but are barely comparable to those of the present study since quite different SOM pools were studied (e.g., Zimmermann et al., 2007; Baldock et al., 2013; Greenberg et al., 2022).

4.3. Benefits of using spiking samples and/or the library

Several authors have reported the relevance of spiking with or without extra-weighting for bias correction and increasing prediction accuracy when large SSLs are used to estimate the soil properties of independent target sets. For example, for SOC or SIC prediction using VNIRS, NIRS or MIRS, the reduction in RMSEP when spiking samples were added with or without extra-weighting could reach 15–20% for local PLSR and 20–90% for global PLSR due to the addition of information from the target site into the calibration dataset (Gogé et al., 2014; Guerrero et al., 2014; Barthès et al., 2020; Ng et al., 2022). This result was in accordance with the results of the present study; considering both calibration procedures, the reduction in RMSEP allowed by spiking and extra-weighting reached 20 to 40% for the non-fractionated soil (20–25% in global calibration, 35–40% in local calibration), 25–30% for F<20, 0% for F20-50, and 10–15% for F>50 (with no clear difference between global and local calibrations for the C amount predictions in the fractions). However, an important result from the present study was that adding SSL to spiking samples did not always improve the predictions of the C amount. Adding SSL improved the prediction in some cases for F<20, F20-50 and F>50 (RMSEP decreased by 0–20%), but not for the non-fractionated soil (RMSEP increased by 0–10%). Ng et al. (2022) studied one VNIR SSL and four target sets in Australia and observed that when SSL was added to the spiking samples, the total SOC prediction was not improved during global calibration, although it was improved during local calibration. On the one hand, the limited benefit provided by the SSL for the C amount predictions could be explained by its limited spectral representativeness of the validation set, as shown in Fig. 3, as a consequence of the nonexhaustive calibration database and strictly independent validation. Thus, the model calibrated with SSL was

partly extrapolated when applied to the validation spectra. On the other hand, adding SSL to the spiking samples could be useful for predicting the C amount in the fractions but not in the non-fractionated soil, possibly because of the uncertainty of conventional determinations. For the C amounts in the fractions, the SEL_{int} was high (cf. Sections 3.4 and 4.6); thus, adding the SSL potentially "diluted" the possible errors in conventional determinations on some spiking samples. In contrast, the SEL_{int} was relatively smaller for the C amount in the non-fractionated soil (ca. 1 gC kg^{-1}; cf. Section 2.3); thus, diluting the possible errors was not necessary.

The benefit of using 15 instead of 10 spiking samples (for a target set of 94 samples) depended on the variable and regression procedure, with no clear trend except that the result was less stable with 10 than 15 spiking samples. Therefore, selecting the appropriate spectral pre-treatment was more challenging with 10 than with 15 spiking samples, but the conventional fractionation of 5 additional samples (i.e., 50% more) was not necessarily justified by its benefit. Barthès et al. (2020) used a national MIR SSL for predicting SIC in a regional target set and observed for both global and local PLSR that increasing the number of spiking samples had no clear benefit beyond a rather low threshold (10 spiking samples for a validation set of 134 samples).

4.4. Benefit of local calibration

Compared with global PLSR, local PLSR did not yield noticeably more accurate predictions (except when predicting the C amount in the non-fractionated soil with target samples alone) and sometimes yielded less accurate predictions (e.g., when predicting the C amount in the non-fractionated soil with SSL alone). This result indicated that global PLSR models were generally as robust as local models since minimal benefit was achieved from the specific calibrations by spectral neighbours. The weak effect of weighting the spectral neighbours in local models could be due to a lack of proximity of the nearest neighbours to the validation samples. In contrast, the spiking samples contained the spectral information from the target set. The use of the spiking samples, either to enrich the SSL or alone, improved both the global and local predictions. The limited benefit of local calibration in these tropical soils contradicts most published results that have addressed such comparisons in temperate areas (Clairotte et al., 2016; Barthès et al., 2020; Cambou et al., 2021; comparisons between Nocita et al., 2014, and Stevens et al., 2013). However, similar prediction results have sometimes been reported. Gomez et al. (2020) used a MIR SSL from France to predict the SOC content in Tunisia; they achieved better predictions with global PLSR model than with local PLSR model when the SOC data were log-transformed (as also done in the present study), but the opposite and poorer predictions were obtained without log-transformation. These authors concluded that correcting the distribution of the response variable (through log-transformation) was more effective than calibrating the model through spectral neighbours to improve prediction accuracy. Therefore, it might be hypothesized that the variable log-transformation also limited the benefits of local calibration in the present study. However, despite the log-transformation of SOC data, Ng et al. (2022) achieved better predictions with the local calibration than with the global calibration when using a VNIR SSL to predict the SOC content in target sets. Thus, by considering our results and published results, no clear conclusion could be drawn, although the prediction of soil organic properties tended to be more accurate in local calibrations when the response variable was not log-transformed and sometimes in global calibrations when it was log-transformed. More research also needs to be performed to address the uncertainty of conventional analysis, which potentially has a greater impact on the accuracy of the local models than on that of the global models when the nearest spectral neighbours are affected.

It should be noted that among the published studies that allowed comparisons between global and local PLSR, few involved spiking, and even fewer involved extra-weighting; moreover, they often concerned temperate areas.

4.5. Differences in the prediction models according to the studied variables

In the present study, when the models were calibrated using SSL with spiking and extra-weighting, the accuracy of the C amount predictions decreased from the non-fractionated soil to F<20 and F>50 and then to F20-50. This was partially in accordance with Barthès et al. (2008), who found better predictions for the non-fractionated soil and F<20 than for F20-50; however, the lowest accuracy was achieved for F50-200 and F200-2000. Ramifehiarivo et al. (2023) also found better predictions of the C amount in F<20 than in the > 50 μm fractions, and explained this result by the different contributions of the fractions to total C; in particular, the fractionation method was unreliable for the fractions > 50 μm due to their low C amounts in the studied Malagasy soils. The same assumption could be made in the present study, as the prediction accuracy was the lowest for F20-50, which contributed the least to the total C amount. Finally, the C amount in F>50 was accurately predicted in the present study, while Barthès et al. (2008) and Ramifehiarivo et al. (2023) reported poor predictions for F50-200 and F>200 separately. This finding indicated that these fractions should not be separately predicted because they were not clearly separated by conventional fractionation and/or by NIRS.

The C amount in each fraction was closely correlated with the C amount in the non-fractionated soil; thus, it could have been assumed that the former was indirectly predicted from the latter. However, the study of the regression coefficients showed strong contributions from both similar and different spectral regions between the fractions and non-fractionated soil (Fig. 5). The regions that strongly contributed to all variables were 1380–1400 nm, 1910–1930 nm, and 2225–2400 nm. The 1380–1400 nm region was assigned to aliphatic organic compounds and water; the 1910–1930 nm region was assigned to water, polysaccharides and carboxylic acids; and the 2225–2400 nm region was assigned to different organic compounds (e.g., polysaccharides and aliphatic organic compounds; Dematte et al., 2006; Rinnan and Rinnan, 2007; Stenberg et al., 2010; Workman and Weyer, 2008). The contribution of these three regions to predict the C amount in the physical (and possibly chemical) fractions has already been reported in the literature (Cozzolino and Morón, 2006; Yang et al., 2012; Greenberg et al., 2022). In contrast, some regions were involved in the prediction of the C amount in the fractions but not in the non-fractionated soil; these regions included the wavelength ranges of 1780–1850 nm, 1888–1896 nm, and 2208–2210 nm and could be assigned to cellulose, carboxylic acids, clay and water (Dematte et al., 2006; Workman and Weyer, 2008). Greenberg et al. (2022) also reported the involvement of different NIR regions when predicting the C amount in the non-fractionated soil and in the studied fractions (e.g., under laboratory conditions, the region at approximately 1400 nm was only important for predicting the fractions). These results strongly suggested that the prediction of the C amount in the fractions was direct, rather than indirect through their correlations with the C amount in the non-fractionated soil, although these correlations were strong.

4.6. Consideration of the effect of the uncertainty of conventional determination on predictions

The prediction accuracy directly depends upon the reliability of reference data used for model calibration, while the *estimation* of NIRS prediction accuracy depends upon the reliability of reference data used for model validation. However, the reliability of reference data has not been extensively studied; few studies have reported replications of SOM fractionation, and most of the time, this information can only be found in Master's or PhD theses. With respect to the SOM fractionations where the dispersion involved beads, HMP and (for the fraction < 50 μm) ultrasonication, the replications mentioned in the limited literature

references (Feller et al., 1991; Razafimbelo, 2002, 2005; Hien, 2004) indicated that for a given sample and fraction, the SD/mean ratio for the fraction C could reach 10% and was sometimes greater than 20% (Table S1). Moreover, replications in each of the cited works were performed by a unique operator; this was also the case for replications carried out on the Togo and southern Benin samples of the present study. In the latter, the fractionation precisions for F<20, F20-50, and F>50 were highly variable: the SD/mean ratio for the C amount in the fractions per duplicated sample ranged from 0.2% to 16% (Table S1). However, over the entire SSL, fractionation was carried out by different operators (one per site in general), and another operator performed most of the fractionation on the target samples. The diversity of operators could increase the variability in the SOM fractionation results. This was confirmed by the high variability of replication results on some target samples, which were carried out by three operators (one per replicate): in each fraction of each sample, the SD/mean calculated for the C amount over the three replicates was at least 10% (in all cases, i.e. in 3 fractions for 3 samples; cf. samples #7 to #9 in Table S1), mostly greater than 20% (6 out of 9 cases), and sometimes greater than 50% (3 out of 9 cases).

Although the limited number of replicates in the present study allowed only a rough estimate of the uncertainty of the SOM fractionation, this uncertainty was high and reflected its potential impact on NIRS prediction accuracy or on the estimation of NIRS prediction accuracy. This is in contradiction with Coates (2002), Sørensen (2002) and Yao et al. (2010) who showed that the degradation of reference data used for calibration generally had a limited effect on the NIRS prediction accuracy during the validation. However, the noise voluntarily added to their reference data by Coates (2002) and Yao et al. (2010) represented at most 10–20% of the mean observation. In the present study, the uncertainty of the reference data represented up to 50% of the mean observation, and SEL_{int} represented at least two-thirds of the RMSEP (Section 3.4). As suggested by Sorensen (2002), when the uncertainty in the reference data (SEL_{int}) is great, it should be removed from the RMSEP using Eq. (6) to accurately evaluate NIRS performance. The uncertainty in reference data used for calibration in the present study could have a great impact on NIRS prediction accuracy, greater than reported by Coates (2002), Sørensen (2002) and Yao et al. (2010). Moreover, a large part of what could be interpreted as insufficient NIRS prediction accuracy could in fact result from the uncertainty of conventional fractionation.

Increasing the number of samples with replicated SOM fractionations could help to improve NIRS predictions. The question arises whether it is preferable (i) to carry out additional SOM fractionations to increase the number of spiking samples or (ii) to carry out additional fractionation replications to improve the quality of reference data. The results of the present study indicated that increasing the number of spiking samples from 10 to 15 had little benefit. Thus, replications of the SOM fractionations would be particularly useful on the calibration samples to improve the accuracy of calibration models. In contrast, replications of reference measurements on validation samples would not affect NIRS predictions (these depend only on the calibration model and on validation spectra), but it would improve the estimation of validation accuracy and the calculation of $RMSEP_{nir}$.

5. Conclusion

In the present work, NIRS data were calibrated using a West African SSL with or without spiking and extra-weighting, and on these spiking samples (i.e., target samples) alone to predict the C amount in the particle size fractions of a local target set in Benin using global (i.e., common) PLSR or more sophisticated local PLSR (calibration by spectral neighbours). Without spiking and extra-weighting, the global models were inaccurate for the non-fractionated soil and F<20 according to $RPIQ_{VAL}$ (between 1.6 and 1.8), but were accurate for F20-50 and F>50 ($RPIQ_{VAL}$ = 1.9). Using a local approach, the models were also inaccurate for the non-fractionated soil and F<20 ($RPIQ_{VAL}$ = 1.6–1.7), and were accurate for F20-50 and F>50 ($RPIQ_{VAL}$ = 1.9–2.1). Therefore, local PLSR could outperform global PLSR in some cases, but the possible benefit was generally limited. Spiking and extra-weighting systematically improved the predictions compared to using the SSL alone, mainly due to a reduction in the bias. In contrast, adding SSL to the target samples was not systematically useful and could even yield poorer predictions than using only target samples for calibration; this was particularly the case for the C amount in the non-fractionated soil. The benefit of adding 15 instead of 10 spiking samples to SSL was often limited and depended on the studied variable and procedure; however, adding 15 instead of 10 samples to SSL generally reduced the variation in prediction accuracy depending on the spectral pretreatment (i.e., raw or pretreated spectra). The consideration of the uncertainty of the conventional determination of fraction C amounts (SEL_{int}), which was noticeable, showed that it could strongly affect the assessment of spectral prediction accuracy; thus, it should be systematically estimated. To date, this has rarely been done in published studies, although conventional determinations, particularly for sandy soils, may lack accuracy. The exclusion of the laboratory uncertainty could lead to underestimate and question the ability of NIRS to predict several variables. The present work opens promising perspectives, as it showed that an SSL consisting of multiregional soil data, with spectral acquisitions spread over 10 years, could enable the accurate prediction of the C amount in the particle size fractions for a new local target set with only a small number of target (spiking) samples to be additionally fractionated. The SSL should continue to be enriched with new samples dissimilar to those already existing in order to progressively gain exhaustiveness.

CRediT authorship contribution statement

Aurélie Cambou: Writing – review & editing, Writing – original draft, Visualization, Validation, Software, Methodology, Formal analysis, Data curation. **Issiakou A. Houssoukpèvi:** Methodology, Validation, Formal analysis, Investigation, Resources, Data curation. **Tiphaine Chevallier:** Writing – review & editing, Supervision, Methodology, Conceptualization. **Patricia Moulin:** Writing – review & editing, Supervision, Methodology, Conceptualization. **Nancy M. Rakotondrazafy:** Validation, Formal analysis, Resources. **Eltson E. Fonkeng:** Methodology, Validation, Formal analysis, Investigation, Resources, Data curation. **Jean-Michel Harmand:** Supervision, Project administration, Writing – review & editing. **Hervé N.S. Aholoukpè:** Supervision, Project administration. **Guillaume L. Amadji:** Supervision, Project administration. **Fritz O. Tabi:** Supervision, Project administration. **Lydie Chapuis-Lardy:** Writing – review & editing, Supervision, Resources, Project administration, Funding acquisition, Conceptualization. **Bernard G. Barthès:** Writing – review & editing, Writing – original draft, Validation, Supervision, Methodology, Data curation, Conceptualization.

Declaration of competing interest

The authors declare that they have no known competing financial interests or personal relationships that could have appeared to influence the work reported in this paper.

Data availability

The authors do not have permission to share data.

Acknowledgements

This work was supported by the SoCa project funded by the Climate Initiative of BNP Paribas Foundation, France. This work also received support from the French National Research Institute for Sustainable Development (IRD, France). The authors acknowledge the joint

international laboratory IESOL for technical assistance. Moreover, the contributions of Rémi d'Annunzio, Moussa Barry, Sofian Conche, Frank Enjalric, Grégoire Freschet, Sophie Lesaint, Joële Louri, and Esso Magamana for SOM fractionations is warmly thanked. Finally, helpful comments from three anonymous Reviewers and Associate Editor are gratefully acknowledged.

Appendix A. Supplementary data

Supplementary data to this article can be found online at https://doi.org/10.1016/j.geoderma.2024.116818.

References

"4 per 1000" Initiative, 2018. URL http://4p1000.org (accessed 7.8.20).
Aholoukpè, H.N.S., 2013. Matière organique du sol et développement du palmier à huile sous différents modes de gestion des feuilles d'élagage : cas des palmeraies villageoises du département du Plateau au Bénin. SupAgro, Montpellier, France. Ph. D. thesis.
Aholoukpè, H.N.S., Amadji, G.L., Blavet, D., Chotte, J.-L., Deleporte, P., Dubos, B., Flori, A., Jourdan, C., 2016. Effet de la gestion des feuilles d'élagage du palmier à huile sur le stock de carbone et les propriétés physico-chimiques du sol dans les palmeraies villageoises du Bénin. Biotechnol Agron Soc Environ 20, 171–182. https://doi.org/10.25518/1780-4507.12946.
Angelopoulou, T., Balafoutis, A., Zalidis, G., Bochtis, D., 2020. From laboratory to proximal sensing spectroscopy for soil organic carbon estimation—A review. Sustainability 12, 443. https://doi.org/10.3390/su12020443.
Azontonde, H.A., 2000. Dynamique de la matière organique et de l'azote dans le système Mucuna-maïs sur un sol ferrallitique (terres de barre) au Sud-Bénin. ENSAM, IRD, Montpellier, France. Ph.D. thesis.
Baldock, J.A., Hawke, B., Sanderman, J., Macdonald, L.M., 2013. Predicting contents of carbon and its component fractions in Australian soils from diffuse reflectance mid-infrared spectra. Soil Research 51, 577–595. https://doi.org/10.1071/SR13077.
Balesdent, J., 1996. The significance of organic separates to carbon dynamics and its modelling in some cultivated soils. Eur J Soil Sci 47, 485–493. https://doi.org/10.1111/j.1365-2389.1996.tb01848.x.
Balesdent, J., Besnard, E., Arrouays, D., Chenu, C., 1998. The dynamics of carbon in particle-size fractions of soil in a forest-cultivation sequence. Plant Soil 201, 49–57. https://doi.org/10.1023/A:1004337314970.
Balesdent, J., Pétraud, J.P., Feller, C., 1991. Effets des ultrasons sur la distribution granulométrique des matières organiques des sols. Science Du Sol 29, 95–106.
Barthès, B.G., Brunet, D., Ferrer, H., Chotte, J.-L., Feller, C., 2006. Determination of total carbon and nitrogen content in a range of tropical soils using near infrared spectroscopy: influence of replication and sample grinding and drying. J near Infrared Spectrosc 14, 341–348. https://doi.org/10.1255/jnirs.686.
Barthès, B.G., Brunet, D., Hien, E., Enjalric, F., Conche, S., Freschet, G.T., d'Annunzio, R., Toucet-Louri, J., 2008. Determining the distributions of soil carbon and nitrogen in particle size fractions using near-infrared reflectance spectrum of bulk soil samples. Soil Biol Biochem 40, 1533–1537. https://doi.org/10.1016/j.soilbio.2007.12.023.
Barthès, B.G., Chotte, J.-L., 2020. Infrared spectroscopy approaches support soil organic carbon estimations to evaluate land degradation. Land Degrad Dev 32, 310–322. https://doi.org/10.1002/ldr.3718.
Barthès, B.G., Kouakoua, E., Coll, P., Clairotte, M., Moulin, P., Saby, N.P., Le Cadre, E., Etayo, A., Chevallier, T., 2020. Improvement in spectral library-based quantification of soil properties using representative spiking and local calibration–The case of soil inorganic carbon prediction by mid-infrared spectroscopy. Geoderma 369, 114272. https://doi.org/10.1016/j.geoderma.2020.114272.
Bellon-Maurel, V., Fernández-Ahumada, E., Palagos, B., Roger, J.-M., McBratney, A., 2010. Critical review of chemometric indicators commonly used for assessing the quality of the prediction of soil attributes by NIR spectroscopy. Trends Analyt Chem 29, 1073–1081. https://doi.org/10.1016/j.trac.2010.05.006.
Boysworth, M.K., Booksh, K.S., 2008. Aspects of multivariate calibration applied to near-infrared spectroscopy, in: Handbook of Near-Infrared Analysis. Burns, D.A., Ciurczak, E.W. (Eds.), third ed., CRC Press, Boca Raton, FL, USA, pp. 207–229. https://doi.org/10.1201/9781420007374-15.
Brandolini-Bunlon, M., Jallais, B., Roger, J.-M., Lesnoff, M., 2023. R package rchemo: Dimension Reduction. Regression and Discrimination for. Chemometrics.
Brown, D.J., Bricklemyer, R.S., Miller, P.R., 2005. Validation requirements for diffuse reflectance soil characterization models with a case study of VNIR soil C prediction in Montana. Geoderma 129, 251–267. https://doi.org/10.1016/j.geoderma.2005.01.001.
Cambou, A., Allory, V., Cardinael, R., Carvalho Vieira, L., Barthès, B.G., 2021. Comparison of soil organic carbon stocks predicted using visible and near infrared reflectance (VNIR) spectra acquired in situ vs. on sieved dried samples: Synthesis of different studies. Soil. Security 5, 100024. https://doi.org/10.1016/j.soisec.2021.100024.
Cambou, A., Barthès, B.G., Moulin, P., Chauvin, L., Faye, E.H., Masse, D., Chevallier, T., Chapuis-Lardy, L., 2022. Prediction of soil carbon and nitrogen contents using visible and near infrared diffuse reflectance spectroscopy in varying salt-affected soils in Sine Saloum (Senegal). Catena 212, 106075. https://doi.org/10.1016/j.catena.2022.106075.
Christensen, B.T., 2001. Physical fractionation of soil and structural and functional complexity in organic matter turnover. Eur J Soil Sci 52, 345–353. https://doi.org/10.1046/j.1365-2389.2001.00417.x.
Clairotte, M., Grinand, C., Kouakoua, E., Thébault, A., Saby, N.P.A., Bernoux, M., Barthès, B.G., 2016. National calibration of soil organic carbon concentration using diffuse infrared reflectance spectroscopy. Geoderma 276, 41–52. https://doi.org/10.1016/j.geoderma.2016.04.021.
Coates, D.B., 2002. Is near infrared spectroscopy only as good as the laboratory reference values? An Empirical Approach. In: Spectroscopy Europe, 24–26. https://www.spectroscopyeurope.com/system/files/pdf/TD_14_4.pdf (accessed 20.10.23).
Cotrufo, M.F., Ranalli, M.G., Haddix, M.L., Six, J., Lugato, E., 2019. Soil carbon storage informed by particulate and mineral-associated organic matter. Nat Geosci 12, 989–994. https://doi.org/10.1038/s41561-019-0484-6.
Cozzolino, D., Morón, A., 2006. Potential of near-infrared reflectance spectroscopy and chemometrics to predict soil organic carbon fractions. Soil Tillage Res 85, 78–85. https://doi.org/10.1016/j.still.2004.12.006.
D'Annunzio, R., Conche, S., Landais, D., Saint-André, L., Joffre, R., Barthès, B.G., 2008. Pairwise comparison of soil organic particle-size distributions in native savannas and Eucalyptus plantations in Congo. For Ecol Manag 255, 1050–1056. https://doi.org/10.1016/j.foreco.2007.10.027.
Dematte, J.A.M., Sousa, A.A., Alves, M.C., Nanni, M.R., Fiorio, P.R., Campos, R.C., 2006. Determining soil water status and other soil characteristics by spectral proximal sensing. Geoderma 135, 179–195. https://doi.org/10.1016/j.geoderma.2005.12.002.
Dignac, M.-F., Derrien, D., Barré, P., Barot, S., Cécillon, L., Chenu, C., Chevallier, T., Freschet, G.T., Garnier, P., Guenet, B., Hedde, M., Klumpp, K., Lashermes, G., Maron, P.-A., Nunan, N., Roumet, C., Basile-Doelsch, I., 2017. Increasing soil carbon storage: mechanisms, effects of agricultural practices and proxies. A Review. Agron Sustain Dev 37, 1–27. https://doi.org/10.1007/s13593-017-0421-2.
Ermer, J., Arth, C., De Raeve, P., Dill, D., Friedel, H.-D., Höwer-Fritzen, H., Kleinschmidt, G., Köller, G., Köppel, H., Kramer, M., Maegerlein, M., Schepers, U., Wätzig, H., 2005. Precision from drug stability studies: Investigation of reliable repeatability and intermediate precision of HPLC assay procedures. J Pharm Biomed Anal 38, 653–663. https://doi.org/10.1016/j.jpba.2005.02.009.
Feller, C., 1979. Une méthode de fractionnement granulométrique de la matière organique des sols – application aux sols tropicaux, à textures grossières, très pauvres en humus. Cahiers ORSTOM, Série Pédologie 17, 339–346.
Feller, C., Beare, M.H., 1997. Physical control of soil organic matter dynamics in the tropics. Geoderma 79, 69–116. https://doi.org/10.1016/S0016-7061(97)00039-6.
Feller, C., Burtin, G., Gerard, B., Balesdent, J., 1991. Utilisation des résines sodiques et des ultrasons dans le fractionnement granulométrique de la matière organique des sols Intérêts Et Limites. Science Du Sol 29, 77–93. https://horizon.documentation.ird.fr/exl-doc/pleins_textes/pleins_textes_5/b_fdi_31-32/34859.pdf (accessed 20.10.23).
Fernández-Ahumada, E., Garrido-Varo, A., Guerrero-Ginel, J.E., Wubbels, A., Van der Sluis, C., van der Meer, J.M., 2006. Understanding factors affecting near infrared analysis of potato constituents. J near Infrared Spectrosc 14, 27–35.
Gavinelli, E., Feller, C., Larré-Larrouy, M.C., Bacye, B., Djegui, N., de Nzila, J.D., 1995. A routine method to study soil organic matter by particle-size fractionation: Examples for tropical soils. Commun Soil Sci Plant Anal 26, 1749–1760. https://doi.org/10.1080/00103629509369406.
Gogé, F., Gomez, C., Jolivet, C., Joffre, R., 2014. Which strategy is best to predict soil properties of a local site from a national Vis–NIR database? Geoderma 213, 1–9. https://doi.org/10.1016/j.geoderma.2013.07.016.
Gomez, C., Chevallier, T., Moulin, P., Bouferra, I., Hmaidi, K., Arrouays, D., Jolivet, C., Barthès, B.G., 2020. Prediction of soil organic and inorganic carbon concentrations in Tunisian samples by mid-infrared reflectance spectroscopy using a French national library. Geoderma 375, 114469. https://doi.org/10.1016/j.geoderma.2020.114469.
Greenberg, I., Seidel, M., Vohland, M., Ludwig, B., 2022. Performance of field-scale lab vs in situ visible/near- and mid-infrared spectroscopy for estimation of soil properties. Eur J Soil Sci 73, e13180. https://doi.org/10.1111/ejss.13180.
Guerrero, C., Stenberg, B., Wetterlind, J., Viscarra Rossel, R.A., Maestre, F.T., Mouazen, A.M., Zornoza, R., Ruiz-Sinoga, J.D., Kuang, B., 2014. Assessment of soil organic carbon at local scale with spiked NIR calibrations: effects of selection and extra-weighting on the spiking subset. Eur J Soil Sci 65, 248–263. https://doi.org/10.1111/ejss.12129.
Guerrero, C., Zornoza, R., Gómez, I., Mataix-Beneyto, J., 2010. Spiking of NIR regional models using samples from target sites: Effect of model size on prediction accuracy. Geoderma 158, 66–77. https://doi.org/10.1016/j.geoderma.2009.12.021.
Hien E., 2004. Dynamique du carbone dans un Acrisol ferrique du Centre Ouest Burkina : Influence des pratiques culturales sur les stocks et la qualité de la matière organique. (Ph.D. thesis) Ecole Nationale Supérieure Agronomique de Montpellier, France.
Houssoukpèvi, I.A., Aholoukpè, H.N.S., Fassinou, D.J.M., Rakotondrazafy, N.M., Amadji, G.L., Chapuis-Lardy, L., Chevallier, T., 2022. Biomass and soil carbon stocks of the main land use of the Allada Plateau (Southern Benin). Carbon Manag 13, 249–265. https://doi.org/10.1080/17583004.2022.2074314.
IUSS (International Union of Soil Science) Working Group WRB (World Reference Base), 2015. World Reference Base for Soil Resources 2014, Update 2015: International Soil Classification System for Naming Soils and Creating Legends for Soil Maps. World Soil Resources Reports, 106, FAO, Rome. https://www.fao.org/soils-portal/soil-survey/soil-classification/world-reference-base/en/.
Jaconi, A., Poeplau, C., Ramirez-Lopez, L., van Wesemael, B., Don, A., 2019. Log-ratio transformation is the key to determining soil organic carbon fractions with near-infrared spectroscopy. Eur J Soil Sci 70, 127–139. https://doi.org/10.1111/ejss.12761.

Kennard, R.W., Stone, L.A., 1969. Computer aided design of experiments. Technometrics 11, 137–148. https://doi.org/10.2307/1266770.
Lal, R., 2014. Soil conservation and ecosystem services. Int Soil Water Conserv Res 2, 36–47. https://doi.org/10.1016/S2095-6339(15)30021-6.
Lavallee, J.M., Soong, J.L., Cotrufo, M.F., 2020. Conceptualizing soil organic matter into particulate and mineral-associated forms to address global change in the 21st century. Glob Chang Biol 26, 261–273. https://doi.org/10.1111/gcb.14859.
Lê, S., Josse, J., Husson, F., 2008. FactoMineR: An R Package for Multivariate Analysis. J Stat Softw 25, 1–18. https://doi.org/10.18637/jss.v025.i01.
Lehmann, J., Kleber, M., 2015. The contentious nature of soil organic matter. Nature 528, 60–68. https://doi.org/10.1038/nature16069.
Li, H., Jia, S., Le, Z., 2020. Prediction of soil organic carbon in a new target area by near-infrared spectroscopy: comparison of the effects of spiking in different scale soil spectral libraries. Sensors 20, 4357. https://doi.org/10.3390/s20164357.
Ludwig, B., Murugan, R., Ramakrishna Parama, V.R., Vohland, M., 2018. Use of different chemometric approaches for an estimation of soil properties at field scale with near infrared spectroscopy. J Plant Nutr Soil Sci 181, 704–713. https://doi.org/10.1002/jpln.201800130.
Mallet, A., Charnier, C., Latrille, É., Bendoula, R., Roger, J.-M., Steyer, J.-P., 2022. Fast and robust NIRS-based characterization of raw organic waste: Using non-linear methods to handle water effects. Water Res 227, 119308. https://doi.org/10.1016/j.watres.2022.119308.
Mark, H., Workman, J.J., 2017. Bias and Slope Correction. Spectroscopy 32, 24–30.
Moni, C., Derrien, D., Hatton, P.-J., Zeller, B., Kleber, M., 2012. Density fractions versus size separates: does physical fractionation isolate functional soil compartments? Biogeosciences 9, 5181–5197. https://doi.org/10.5194/bg-9-5181-2012.
Ng, W., Minasny, B., Jones, E., McBratney, A., 2022. To spike or to localize? Strategies to improve the prediction of local soil properties using regional spectral library. Geoderma 406, 115501. https://doi.org/10.1016/j.geoderma.2021.115501.
Nocita, M., Stevens, A., Toth, G., Panagos, P., van Wesemael, B., Montanarella, L., 2014. Prediction of soil organic carbon content by diffuse reflectance spectroscopy using a local partial least square regression approach. Soil Biol Biochem 68, 337–347 https://doi.org/j.soilbio.2013.10.022.
O'Rourke, S.M., Holden, N.M., 2011. Optical sensing and chemometric analysis of soil organic carbon – a cost effective alternative to conventional laboratory methods? Soil Use Manag 27, 143–155. https://doi.org/10.1111/j.1475-2743.2011.00337.x.
Pansu, M., Gautheyrou, J. (Eds.), 2006a. Physical Fractionation of Organic Matter, in: Handbook of Soil Analysis: Mineralogical, Organic and Inorganic Methods. Springer, Berlin, Heidelberg, pp. 289–326. https://doi.org/10.1007/978-3-540-31211-6_9.
Pansu, M., Gautheyrou, J. (Eds.), 2006b. Particle Size Analysis, in: Handbook of Soil Analysis: Mineralogical, Organic and Inorganic Methods. Springer, Berlin, Heidelberg, pp. 15–63. https://doi.org/10.1007/978-3-540-31211-6_2.
Peterson, B.G., Carl, P., 2020. PerformanceAnalytics: Econometric Tools for Performance and Risk Analysis.
Poeplau, C., Don, A., Six, J., Kaiser, M., Benbi, D., Chenu, C., Cotrufo, M.F., Derrien, D., Gioacchini, P., Grand, S., Gregorich, E., Griepentrog, M., Gunina, A., Haddix, M., Kuzyakov, Y., Kühnel, A., Macdonald, L.M., Soong, J., Trigalet, S., Vermeire, M.-L., Rovira, P., van Wesemael, B., Wiesmeier, M., Yeasmin, S., Yevdokimov, I., Nieder, R., 2018. Isolating organic carbon fractions with varying turnover rates in temperate agricultural soils – A comprehensive method comparison. Soil Biol Biochem 125, 10–26. https://doi.org/10.1016/j.soilbio.2018.06.025.
Ramesh, T., Bolan, N.S., Kirkham, M.B., Wijesekara, H., Kanchikerimath, M., Rao, C.S., Sandeep, S., Rinklebe, J., Ok, Y.S., Choudhury, B.U., Wang, H., Tang, C., Wang, X., Song, Z., Freeman II, O.W., 2019. Chapter One - Soil organic carbon dynamics: Impact of land use changes and management practices: A review. Adv Agron 156, 1–107. https://doi.org/10.1016/bs.agron.2019.02.001.
Ramifehiarivo, N., Barthès, B.G., Cambou, A., Chapuis-Lardy, L., Chevallier, T., Albrecht, A., Razafimbelo, T., 2023. Comparison of near and mid-infrared reflectance spectroscopy for the estimation of soil organic carbon fractions in Madagascar agricultural soils. Geoderma Regional 33, e00638. https://doi.org/10.1016/j.geodrs.2023.e00638.
Razafimbelo, T., 2002. Effet du non-brûlis de la canne à sucre sur la séquestration de C dans un sol ferrallitique argileux (Brésil). Institut National Agronomique Paris-Grignon, France. MsC thesis.
Razafimbelo, T., 2005. Stockage et protection du carbone dans un sol ferrallitique sous systèmes en semis direct avec couverture végétale des Hautes Terres malgaches. Ecole Nationale Supérieure Agronomique de Montpellier, France. Ph.D. thesis.
Rinnan, R., Rinnan, Å., 2007. Application of near infrared reflectance (NIR) and fluorescence spectroscopy to analysis of microbiological and chemical properties of arctic soil. Soil Biol Biochem 39, 1664–1673. https://doi.org/10.1016/j.soilbio.2007.01.022.
Rubel, F., Kottek, M., 2010. Observed and projected climate shifts 1901–2100 depicted by world maps of the Köppen-Geiger climate classification. Meteorologische Zeitschrift 19, 135–141. https://doi.org/10.1127/0941-2948/2010/0430.
Sauvadet, M., Saj, S., Freschet, G.T., Essobo, J.-D., Enock, S., Becquer, T., Tixier, P., Harmand, J.-M., 2020. Cocoa agroforest multifunctionality and soil fertility explained by shade tree litter traits. J Appl Ecol 57, 476–487. https://doi.org/10.1111/1365-2664.13560.
Shahbazikhah, P., Kalivas, J.H., 2013. A consensus modeling approach to update a spectroscopic calibration. Chemometr Intell Lab Syst 120, 142–153. https://doi.org/10.1016/j.chemolab.2012.06.006.
Sørensen, L.K., 2002. True accuracy of near infrared spectroscopy and its dependence on precision of reference data. J near Infrared Spectrosc 10, 15–25. https://doi.org/10.1255/jnirs.317.
Stenberg, B., Viscarra Rossel, R.A., Mouazen, A.M., Wetterlind, J., 2010. Visible and near infrared spectroscopy in soil science. Adv Agron 107, 163–215. https://doi.org/10.1016/S0065-2113(10)07005-7.
Stevens, A., Nocita, M., Tóth, G., Montanarella, L., van Wesemael, B., 2013. Prediction of soil organic carbon at the European scale by visible and near infrared reflectance spectroscopy. PLoS ONE 8, e66409. https://doi.org/10.1371/journal.pone.0066409.
Stevens, A., Ramirez-Lopez, L., 2022. An introduction to the prospectr package. R Package Vignette R Package Version (2), 5.
Von Lützow, M., Kögel-Knabner, I., Ekschmitt, K., Flessa, H., Guggenberger, G., Matzner, E., Marschner, B., 2007. SOM fractionation methods: Relevance to functional pools and to stabilization mechanisms. Soil Biol Biochem 39, 2183–2207. https://doi.org/10.1016/j.soilbio.2007.03.007.
Wold, S., Martens, H., Wold, H., 1983. The multivariate calibration problem in chemistry solved by the PLS method. In: Kågström, B., Ruhe, A. (Eds.), Matrix Pencils, Lecture Notes in Mathematics. Springer, Berlin, Heidelberg, pp. 286–293. https://doi.org/10.1007/BFb0062108.
Workman Jr., J.J., 2007. NIR spectroscopy calibration basics. In: Press, C.R.C. (Ed.), Handbook of near-Infrared Analysis, 3rd Edition. Boca Raton, Floride, USA, pp. 123–151.
Workman Jr., J., Weyer, L., 2008. Practical Guide to Interpretive Near-Infrared Spectroscopy, first ed. CRC Press, Boca Raton, FL, USA.
Yang, X.M., Xie, H.T., Drury, C.F., Reynolds, W.D., Yang, J.Y., Zhang, X.D., 2012. Determination of organic carbon and nitrogen in particulate organic matter and particle size fractions of Brookston clay loam soil using infrared spectroscopy. Eur J Soil Sci 63, 177–188. https://doi.org/10.1111/j.1365-2389.2011.01421.x.
Yao, S., Xing, M., Zhou, S., Wu, G., Jiang, Y., Pu, J., 2010. The accuracy of near infrared prediction of hemicellulose content arising from varying introduced errors. J near Infrared Spectrosc 18, 397–402. https://doi.org/10.1255/jnirs.908.
Zimmermann, M., Leifeld, J., Fuhrer, J., 2007. Quantifying soil organic carbon fractions by infrared-spectroscopy. Soil Biol Biochem 39, 224–231. https://doi.org/10.1016/j.soilbio.2006.07.010.